2019

DISCOVERY OF SELECTIVE PROBES TARGETING RNA POLYMERASE I

Xiao Tan
University of Kentucky, thisixt0813@gmail.com
Author ORCID Identifier:
https://orcid.org/0000-0003-3283-7780
Digital Object Identifier: https://doi.org/10.13023/etd.2019.259

STUDENT AGREEMENT:

I represent that my thesis or dissertation and abstract are my original work. Proper attribution has been given to all outside sources. I understand that I am solely responsible for obtaining any needed copyright permissions. I have obtained needed written permission statement(s) from the owner(s) of each third-party copyrighted matter to be included in my work, allowing electronic distribution (if such use is not permitted by the fair use doctrine) which will be submitted to UKnowledge as Additional File.

I hereby grant to The University of Kentucky and its agents the irrevocable, non-exclusive, and royalty-free license to archive and make accessible my work in whole or in part in all forms of media, now or hereafter known. I agree that the document mentioned above may be made available immediately for worldwide access unless an embargo applies.

I retain all other ownership rights to the copyright of my work. I also retain the right to use in future works (such as articles or books) all or part of my work. I understand that I am free to register the copyright to my work.

REVIEW, APPROVAL AND ACCEPTANCE

The document mentioned above has been reviewed and accepted by the student's advisor, on behalf of the advisory committee, and by the Director of Graduate Studies (DGS), on behalf of the program; we verify that this is the final, approved version of the student's thesis including all changes required by the advisory committee. The undersigned agree to abide by the statements above.

Xiao Tan, Student

Dr. Samuel G. Awuah, Major Professor

Dr. Mark A. Lovell, Director of Graduate Studies

DISCOVERY OF SELECTIVE PROBES TARGETING RNA POLYMERASE I

THESIS

A thesis submitted in partial fulfillment of the
requirements for the degree of Master of Science in the
College of Arts and Sciences
at the University of Kentucky

By

Xiao Tan

Lexington, Kentucky

Director: Dr. Samuel G. Awuah, Professor of Chemistry

Lexington, Kentucky

2019

https://orcid.org/0000-0003-3283-7780

ABSTRACT OF THESIS

DISCOVERY OF SELECTIVE PROBES TARGETING RNA POLYMERASE I

RNA Polymerase I (RNA Pol I) is a "factory" that orchestrate the transcription of ribosomal RNA for constructing ribosomes as a primary workshop for protein translation to sustain cell growth. Deregulation of RNA Pol I often cause uncontrolled cell proliferation leading to cancer. Efficient and reliable methods are needed for the identification of selective inhibitors of RNA Pol I. Yeast (*Saccharomyces cerevisiae*) is eukaryotic and represent a valuable model system to study RNA Pol I, especially with the availability of the X-ray crystal structure of the yeast homologue of RNA Pol I, offering structural basis to selectively target this transcriptional machinery. Herein, we developed a cell-based screening strategy by establishing a stable yeast cell line with stably integrated human RNA Pol I promoter and ribosomal DNA. The model system was validated using the well-known RNA Pol I inhibitor, CX-5461 by measuring the transcribed human rRNA as a readout. Virtual screening coupled with compound library screening using this cell line enabled the identification of a new candidate inhibitor of RNA Pol I, cerivastatin sodium. Furthermore, we used growth assays and gel electrophoresis, to biologically evaluate the hit. The result implicates cerivastatin sodium as a selective RNA Pol I inhibitor worthy of further development with potential as targeted anticancer therapeutic.

KEYWORDS: RNR Polymerase I, Yeast, Cerivastatin Sodium, CX5461, YIPlac211-TG1, YBR140C.

Xiao Tan
(Name of Student)

06/24/2019
Date

DISCOVERY OF
SELECTIVE PROBES TARGETING RNA POLYMERASE I

By
Xiao Tan

Samuel G. Awuah
Director of Thesis

Mark A. Lovell
Director of Graduate Studies

06/24/2019
Date

DEDICATION

To my father Daqing Tan and my mother Meiting Yao,
I appreciate your care and love forever. Without them I could not have achieved what I have.

ACKNOWLEDGMENTS

The following thesis, while an individual work, benefited from the insights and direction of several people. First, my Thesis Chair, Dr. Samuel G. Awuah, exemplifies the high quality scholarship to which I aspire. In addition, Dr. Brian G. Rymond provided essential instruction and bio-material support, allowing me to complete my project. Next, I appreciate Dr. Yinan Wei for her warmhearted guidance during my major difficulty as well as the significant material support for me to run experiments with protein and first DNA extraction. I wish to thank the complete Thesis Committee, respectively: Dr. Yinan Wei, and Dr. Louis B Hersh. Each individual provided insights that guided and challenged my thinking, substantially improving the finished product. We thank the NCATS program for small molecule library.

In addition to the technical assistance above, I received equally important assistance from family and friends. Finally, I wish to thank the respondents of my study.

TABLE OF CONTENTS

LIST OF TABLES

LIST OF FIGURES

CHAPTER 1. INTRODUCTION

1.1 Background Knowledge of RNA Polymerase I

1.1.1 Myc Gene Family and RNA Polymerases

The Myc gene family includes a couple of proto-oncogenes coding for transcription factors. Overexpression of proto-oncogenetic *Myc* genes was determined to cause cancer development in studies of diverse organs including intestine by Kim et al (2018)[1] , testicular by Corbineau et al (2017)[2], liver by Zhao el al (2016)[3], etc. Study using multiple cell strains by Ji et al (2011)[4] has shown that activated MYC genes induce cell mass accumulation and cell proliferation. This stimulation of cell growth heavily depends on production of ribosome as well as transcription and maturation of multiple types of RNAs, both of which are intensely supported by the activities of RNA polymerases.

In eukaryotes, RNA Pol II is a nucleoplasm polymerase that produces mRNAs for supplying cells growth with proteins. Transcription activities of RNA Pol III yield 5s rRNA, tRNA and small sized non-coding RNAs that involve with metabolism, which had been studied by Roeder et al (1969)[5]. In comparison, eukaryotic RNA Pol I is localized in nucleoli and its specific DNA template to work on is ribosomal DNA. Transcription of rDNA by RNA Pol I yields 47S pre-rRNA, which is subsequently processed into 18 S, 5.8 S and 28 S rRNAs[5] [6] as depicted in (Figure 1.1**)**. These rRNAs are important building materials for ribosome, which is the organelle for synthesizing new proteins[7]. Analysis by Fernandez-Tornero et al (2013)[8] showed that RNA Pol I is a multi-subunit enzyme that had 14 subunits. In comparison, RNA Pol II possess 10 subunits[9].

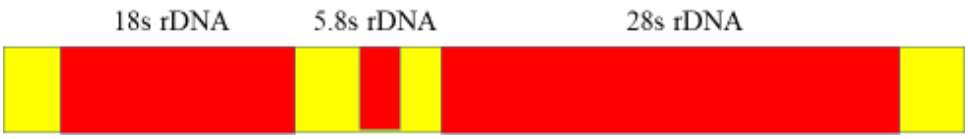

Figure 1.1 Structure of a Single Repeat of Yeast Ribosomal DNA

1.1.2 Structure and Functions of rDNA as RNA Pol I's Template

As the template for RNA Pol I, eukaryotic rDNA of both human and yeast have multiple copies of rDNA sequences. Yeast genome contains 150 to 200 repeats of rDNA within chromosome XII[10] whereas human beings have about 400 copies of rDNA repeats that are distributed in five chromosomes[11].

As one copy of the multiple repeats, a typical rDNA for eukaryotes includes three significant components: proximal promoter[12], enhancers[13] and space-promoters and terminators[14]. Proximal promoter is needed for sequence-specific initiation of rDNA transcription[12]. Experiments of point mutation and sequence deletion within the promoter regions of the mouse rDNA at different distances from the transcription starting point of the rDNA suggested it was proximal promoter (Figure 1.2) that controlled the initiation of rDNA transcription[12 15].

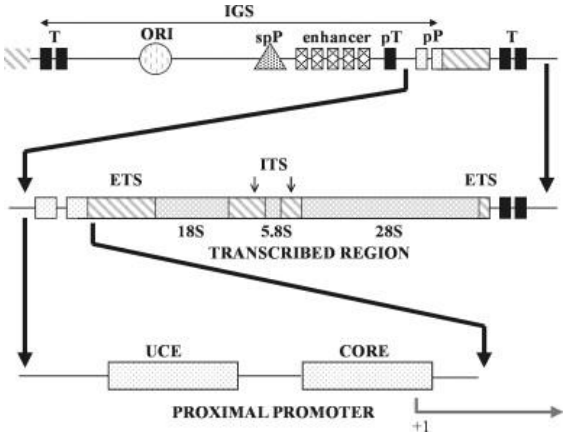

Figure 1.2 Structure of a Single Repeat of Yeast Ribosomal DNA (rDNA)

1.1.3 Structure of RNA Pol I for Yeast and Human RNA Pol I

RNA Pol I of Yeast (*Saccharomyces cerevisiae*) is a multi-subunit enzyme and its crystallized structure reveals 14 subunits that are originally named as A190/ RPA190, A135/ RPA135, AC40, A14, ABC27, ABC23, A43, ABC14.5, A12.2, ABC5, RPA19/ AC19, ABC4, A49, A34.5 [16] [17]. A 3D structure of Yeast RNA Pol I in complex with RRN3 at a resolution at 4.8 angstrom has been published by Russell and Zomerdijk (2006)[17] as shown by (Figure 1.3). The file documenting this protein complex is deposited in Protein Data Bank with the referable code of 5g5l, of which the subunites were depicted in (Figure 1. 4)[17]. The subunits collaborate in sustaining the structure or functioning for specific processes of rDNA transcription. Of all these subunits, the RNA Pol I subunits A190, A135 and A12.2 are also referred to as RPA194, RPA135 and RPA12 and were determined to constitute the catalytically active center including the DNA binding cleft[8]. A serial combination of protein expression using plasmids containing cDNA, chromatographic extraction using His-tag, using resolution by SDS-PAGE and interaction assay reported using autoradiography done by Peyroche et al (2002)[18] had revealed a strong interaction between RNA Pol I subunit A43 and A14. Such a interaction was strong enough to hold this two subunits within a complex[19].

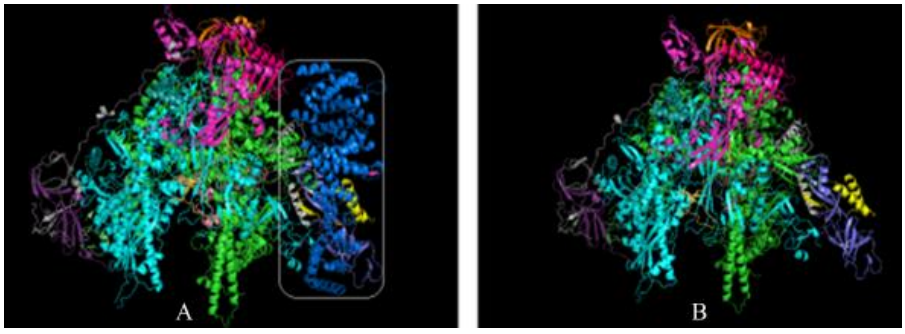

Figure 1.3 Yeast RNA Pol I with and without Contact Presence of RRN3

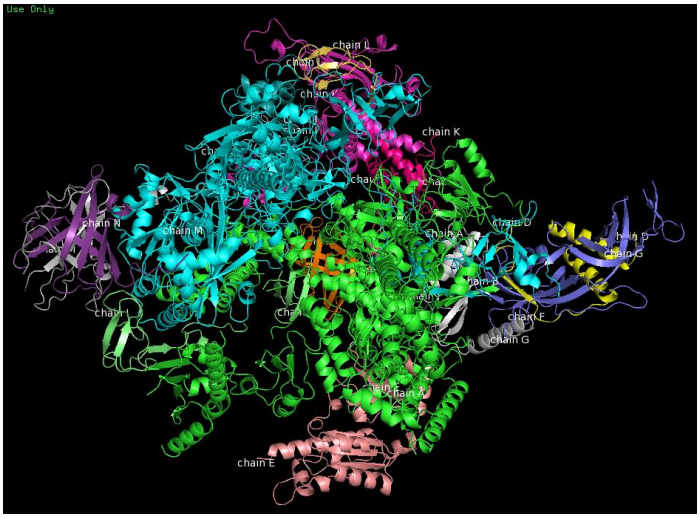

Figure 1.4 Structure of Yeast RNA Pol I

The 3D structural images of RNA Pol I obtained from cryo EM by Tafur et al (2016)[20] provide direct evidence as well as structural depiction of A43 as a mediator that recruit two RNA Pol I enzymes to form a dimerization. Their data also described a bridge helix (BH) formed by Amino Acid Residues 1012-1016 of subunit RPA190. Their data described how BH either contract or extend in order to close or open the DNA binding cleft. Ultimately their results clarified and how structural changes within RPA190 could switching RNA Pol I from one dynamic structure within the opening complex to another within the elongation complex during the transcription cycle.

1.2 RNA Polymerase I as a Promising Anti-Cancer Target

The characteristic fast proliferation of cancer cells strongly replies a much higher capacity of cellular protein synthesis. To compensate for protein errors and loss cancer cells are pressured into increased protein synthesis at higher levels[21]. Such a reliance for fast protein synthesis in turn heavily depends on construction of new ribosomes, of which rRNA synthesized by RNA Pol I is a significant building material. Prior research also

showed that for the cellular levels of ribosome the accessibility of rRNA is a significant determinant [22].

Moreover, the RNA Pol I transcription constitutes up to 60 % of all cellular transcription among the three RNA polymerases, and rRNAs make up about 80 % of the RNA content of living cells[23]. Therefore, RNA Pol I is crucial in controlling cell growth and its misregulation is associated with aberrant cell growth and thus increased risk of cancer. Study by Bywater et al (2012)[24] reported the direct cellular evidence for enhanced ribosomal DNA transcription levels by increased RNA Pol I activity as a cause of cancer progression. The same study also lend evidence that selective inhibition of RNA Pol I could contribute to apoptosis of specific human malignant cells like lymphoma cells and thus is a promising therapy against cancer. Inhibitors to the rDNA transcription function of RNA Pol I could probably suppress growth of cancer cells and thus be used as targeted anti-cancer drugs[25].

1.3 Challenges in Obtaining Selective Inhibitors to RNA Pol I

RNA Pol I remains an important target for anti-cancer therapy that screening and designing specific inhibitors to this enzyme is valuable. However, this goal is challenging for a couple of reasons.

First, the high structural similarity shared by all three RNA polymerases might make it difficult to achieve small molecule selectivity. Structural comparison done by Cramer et al of all three RNA polymerases reveals highly conserved active site[26]. Identified RNA Pol I inhibitors screened based on blockage of substrate (DNA) access to the catalytic active site, opens the possibility for such an inhibitor to simultaneously inhibit either or both of the other counterpart polymerases.

The second challenge is the lack of high-throughput assay methods to quantify rRNA, which is the product of RNA Pol I catalysis. Multiple challenges therefore exist in

monitoring rRNAs transcribed by RNA Pol I following treatment of compound libraries. A major limitation is the short half-life of rRNA, which is ~20 and 30 minutes and sensitive to degradation[27]. Therefore, resultant RNA extracts must be handled strictly in RNase and nucleotide free buffers during their extraction and storage. Were the transcription quantified directly using reverse transcription qRT-PCR assay, the operation would be laborious and require stringent operation conditions in order to generate accurate and precise data. The third reason is that there has not been a fully elucidated x-ray crystal structure of Human RNA Pol I. Therefore, it requires designing a persuasive protein model to identify candidate compounds targeting human RNA Pol I.

Moreover, it is important to take into account selective RNA Pol I probes or inhibitors that are safe to normal functions of healthy cells. Some effective anticancer drugs, targeting RNA Pol I may also have unpleasant side effects leading to high cellular toxicity[28] as exemplified in Actinomycin D in (Figure 1.5). This well-known anticancer drug lacks selectivity against RNA Pol I and has been shown to inhibit RNA Pol II[27]. This drug, therefore, might be disadvantageous to normal cellular function like protein synthesis. More innovative screening approaches to access selective RNA Pol I inhibitors are needed.

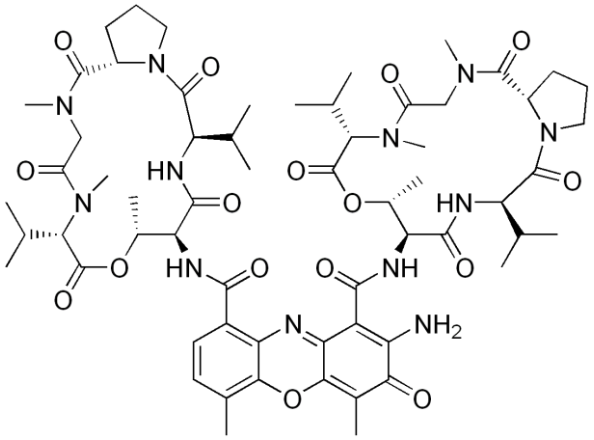

Figure 1.5 Structure of Actinomycin D

1.4 Unique Structural Hints of RNA Pol I for Inhibitor Design

To overcome the outlined drawbacks (*vide supra*) that limit rational design of potent specific RNA Pol I inhibitors, novel concepts with important compatible screening methods are required. Identification of such inhibitors require comprehensive knowledge of the precise structures of RNA Pol I as well as other macro biomolecules that closely interact with the RNA Pol I in the whole process of transcription and its regulation.

1.4.1 Regulatory Factors of RNA Pol I for Yeast and Human

For human RNA Pol I there are two important factors, Upstream Binding Factor (UBF) and Selective Factor 1 (SL1) that bind the promoter region of human rDNA, recruit the other molecules that participate in the formation of transcription complex (Figure 1. 6). SL1 interacts with promoter DNA in a highly sequence-specific manner as illustrated (Figure 1. 6) by the sequence-specific nature of rDNA onto sequences from upstream promoter element and core promoter element during initiation of transcription [29] [30] [31]. The counterpart factor of SL1 in yeast is TIF-1B; the two factors differ in that binding of SL1 to human rDNA promoter requires UBF whereas the TIF-1B binds with yeast rDNA promoter in the absence of UBF [29]. These structural distinctions can be further exploited to obtain RNA Pol I specific small molecule inhibitors.

Another important regulatory factor for RNA Pol I is RPA53. Recent research showed this acetylation as well as de-acetylation of a specific lysine residue on this factor could increase or decrease the transcription activity of rDNA[32].

1.4.2 Protein Factors Having Direct Contact with RNA Pol I

There are a couple of protein factors that regulate the transcription activity of RNA via direct contact. One of these transcription factors, Rrn3 was identified as a

unique binding factor[33] that directly interacted with Yeast RNA Pol I to form an initiation complex. Their investigation also showed Rrn3 would specially recognize sequences of Yeast rDNA and recruit RNA Pol I to that promoter region. This process is noticeable in being independent of the rDNA sequence. Rrn3 ultimately recruits RNA Pol I to the specific rDNA promoter regions [34]. Later investigations[35] showed that Rrn3 binds RNA Pol I as a monomer. Characterization of the interfaces between RNA Pol I and Rrn3 would probably provide with valuable information for designing RNA Pol I inhibitors based on destabilization of the complex formed by these two biomolecules. The surface image of average position depicted by the immunolocalization experiment[18] provided direct evidence for the formation of a complex of A43 from RNA Pol I and Rrn3 as depicted in (Figure 1.6).

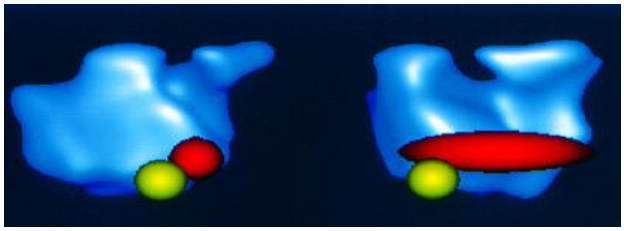

Figure 1.6 Surface Image Model of Yeast RNA Pol I

Investigation by Blattner et al (2011) [35] showed a serine (S154) patch on the interface between Rrn3 and RNA Pol I during the formation of transcription complex. Once this serine (S154) was phosphorylated, binding between Rrn3 and RNA Pol I would be suppressed. This blockage would in turn inhibit RNA Pol I's transcription activity as well as cell growth [35]. This provides with significant hint for inhibitor design. Because the serine patch on Rrn3 fits in the site formed between two RNA Pol I subunits: AC 40/19 and A14/43 while binding takes place, screening compounds that have high affinity to this binding site may be possible.

Experimentally virtual screening can be done using the known structural data of RNA Pol I and its specific transcription factors. Molecular docking using programs including Autodock and SYBYL-X can be carried out for the structural data of RNA Pol I with the virtual structural files of compound candidates.

Our project hypothesizes that compounds that can destabilize the complex formed between the apozyme of Pol I and Rrn3 can be a potential selective inhibitor to RNA Pol I function and thus be used as anti-cancer drugs.

1.5 Prior Researches about Selective Inhibitors to RNA Pol I

Bio-models containing the source of RNA Pol I are indispensable for assaying this enzyme's activity. Prior researches had adopted diverse systems such as diverse cancer cell lines, cellular extract and purified RNA Polymerases as source of RNA Pol I to design activity assays. For the activity assays the design for quantifying the enzyme activity is a major concern for assessing the inhibitory potency of the ligands to be tested. Once a potential inhibitor is screened, a selectivity test is necessary for assessing its value as a drug candidate. Usually a Pol I inhibitor is expected not to inhibit Pol II at the dose with therapeutic efficacy in order not to disturb the desired function of RNA Pol II in transcription of the house keeping genes, which would yield the mRNA for the functional proteins like enzymes.

1.5.1 Prior Bio-Models Assaying RNA Pol I

Screening the experimental hit of selective inhibitors to RNA Pol I requires efficient design of a bio-system containing RNA Pol I as well as other protein factors, as well as the template DNA containing the rDNA and promoter. These constitute the

molecular basis for an assay to quantify the transcription activity of RNA Pol I. The cell system assaying RNA Pol I were usually human cancer cells because their levels of RNA Pol I transcription activities were high. Prior studies used diverse lines with advantages that were desirable for anti-cancer drugs' development. One of such cell lines was the NCI60 cell lines [36] [37]. Another cell line was HeLa S3 which could form colonies much more easily at relatively lower concentrations of nutrient supply such as human serum and formed bigger and more stable colonies than other strains of Hela cells[38]. Cell lines from Eμ-*Myc* B These cell lines were selected and cultured for the purpose of screening anti-cancer drugs via inhibition to the cell's proliferation.

In other bio-model of RNA Pol I study used lines of lymphoma cells like murine Eμ-*Myc*-lymphoma cells and Eμ-Myc-B cells [39] because these cell lines demonstrated high levels of protein factors for RNA Pol I's transcription high levels of rDNA transcription. Therefore, these cell lines could generate more evident signals of proliferation inhibition with presence of inhibitors as anticancer drugs like CX-5461 (Figure 1.7) and provide with a desirable comparison with RNA Pol I inhibitors to be studied [24]. In the same research, a comparison in dose dependent tests between malignant B cells and the wild type B cells revealed that CX54-61 also selectively suppress the B-lymphoma cells that were cancerous target [24].

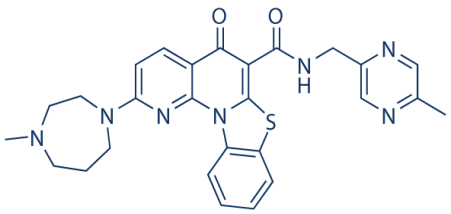

Figure 1.7 Structure of CX-5461

HepG2 cells had also been used for building an rDNA transcription assay by Ghoshal et al (2004) [11] with the firefly luciferase as the reporter enzyme for RNA Pol I transcription. This cell line was probably more desirable as the host for RNA Pol I driven transcription that was assayed using reporter enzymes since the data showed HepG2 cell had higher luciferase activity driven by RNA Pol I transcription than Hela cells.

There are many published methods that reported bio-models assaying RNA Pol I activity using cancer cell extracts instead of whole cancer cells. Kurl et al (1984) [40] had successfully transcribed rat rDNA using rat mammary adenocarcinoma ascites cells as the start to make such a cell-free in vitro assay. Their work obtained two chromatographic fractions with DEAE-Sephadex column and tandem fraction combining both DEAE-Sephadex column and heparin-Sepharose column from rat cells that could yield an over 90 percent of RNA Pol I transcription activity. Their work showed that a cellular extract could concentrate RNA Pol I through chromatographic fraction with DEAE-Sephadex column followed by a second round of fraction through heparin-Sepharose column chromatography. Furthermore, the following fractionation using heparin-Sepharose column chromatography turned out to increase the extract's RNA Pol I transcription activity. Interestingly, chromatographic phosphocellulose was suggested not to be used during the early phase of fractionation in order to prevent from the loss of activity in rDNA transcription. Except for a source of RNA Polymerase I, another essential component for the bio-system assaying rDNA transcription was a template DNA containing rDNA together with an adjacent promoter. Such a template could be the rDNA plus promoter within a whole cell's intact genome. It also could be a DNA sequence containing the rDNA of interest plus rDNA promoter that were cut out directly

from a creature's genome. It could also be a recombined plasmid containing the rDNA with promoter. Ghoshal et al (2004)[11] had constructed an rDNA template as a plasmid named as pHrD-IERS-Luc in which luciferase reporter was in a tandem followed by an IRES-human rDNA sequence. This project discovered that methylation of the nucleotides constituting the rDNA promoter would weaken the transcription of rDNA catalyzed by RNA Pol I.

Prior studies had developed multiple assays quantifying RNA Pol I activity. Direct quantification had been done reverse transcription qRT-PCR assay using the 45S rRNA as the RNA template and nuclear extract from HeLa S3 cells as the RNA Pol I source in one project investigating CX-4561 as RNA Pol I inhibitor [41]. Indirectly quantifying the rDNA transcription activity of RNA Pol I by activity of a reporter enzyme had been an existing strategy. For example, Ghoshal et al (2004)[11] had designed an in vitro assay to quantify Human rDNA transcription activities using firefly luciferase as illustrated in (Figure. 1.8**)**.

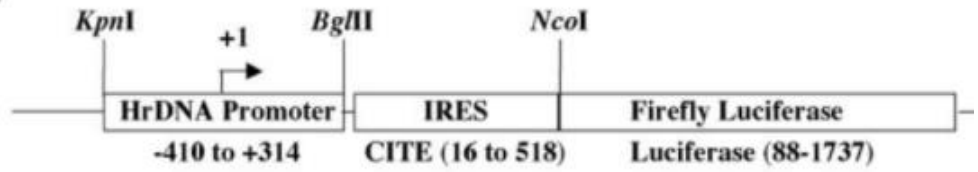

Figure 1.8 Construction of pHrD-IRES-Luc Plasmid

1.5.2 Studies of Interaction between RNA Pol I and Inhibitors

Another concern of RNA Pol I study is the molecular mechanism via which each inhibitor act on RNA Pol I. Several inhibitors were verified to work exclusively by disturbing the formation of transcription complex and do not directly degrade the cancer cells. For instance, research with a compound called CX-5461 implicated it was a

potential anticancer drug candidate against development of diverse cancer tissues by inducing cancer cells' autophagy, senescence as well as by inhibiting the transcription activity of RNA Pol I via blockage against the formation of transcription initiation complex [41] [24]. It is also noticeable that CX-5461 was concluded as acting in an independent of P53 pathway and was able to induce apoptosis[41]. Similarly, another drug called 9-Hydroxyellipticine was shown as a disturber of the interaction between Human rDNA promoter and SL1 during the formation of preinitiation complex[42]. Research by Colis et al (2014) [25] had investigated pyridoquinazolinecarboxamides and its derivatives as RNA Pol I inhibitors. BMH-21 was also found to be a potent RNA Pol I inhibitor that could block the RNA Pol I holocomplex from binding to rDNA and thus inhibit the RNA Pol I's transcription activity[43]. In the same project a series of BMH-21 derivatives were synthesized and tested in rDNA transcription activity assay. A comparison showed that the BMH-21 compound series all intercalated with rDNA but only 12H-benzo[g] pyrido [2,1-b] quinazoline-4-carboxamide, N-[2 (dimethylamino) ethyl]-12-oxo, which they named as BMH-21(2). Their study used NCI60 human tumor cell line [37] and successfully demonstrated that BMH-21 competed with RNA Pol I for the GC region binding site of the human rDNA instead of contacting with the active site on the surface of RNA Pol I. Moreover, the same research found BMH-21 could degrade RBP194 subunit of RNA Pol I [43] and thus block the formation of initiation complex in an alternative strategy as compared to CX-5461.

1.5.3 Selectivity of RNA Pol I Inhibitors to Growth of Cancer Cells

Nucleolin as another RNA Pol I inhibitor, was studied in both inhibitory potency and selectivity by Roger et al. Their work showed nucleotin could suppress transcription

of rDNA by RNA Polymerase I whereas function of RNA Pol II and Pol III remained unaffected. Nucleolin was concluded to inhibit RNA Pol I via direct disturbance of Pol I's interaction with rDNA and depended specially on the sequence of promoter instead of pre rDNA[44]. Andrews et at (2013)[42] had conducted study that focused on finding selective RNA Pol I inhibitors from old drugs using a couple of human cell strains. They used three transcription assays targeting rDNA for RNA Pol I, a group of housekeeping genes targeting RNA Pol II and 5s plus 7s rDNA targeting RNA Pol III. These strict screening identified a highly efficient and selective RNA Pol I inhibitor from the ellipticine family: 9-Hydroxyellipticine (9HE). Impressively they had also conducted a series of other assays with anticancer drug targets including p53, ATM/ATR, and Top2 and found that none of these were affected by 9HE.

1.6 Basis of Using Yeast RNA Pol I to Anticancer Drugs' Design

Yeast (Saccharomyces cerevisiae) has become a model for investigating complex molecular genetic processes like transcription of eukaryotes that are multicellular because it is easy to process [45] and the conservation in protein functions between yeast and other eukaryote like human beings [46] [45] [47]. Yeast RNA Pol I is also the only eukaryote of which the RNA Pol I's structure has been fully characterized.

For Saccharomyces cerevisiae (Yeast) RNA Pol I exclusively works on 35s rDNA[48]. Sequence alignments done using a couple mammalian RNA Pol I subunits (cloned using their cDNAs) with their counterpart subunits from in yeast RNA Pol I indicated high homology[49]. Moreover, experiments also showed four subunits were functionally interchangeable between human and yeast. Therefore, in our project a

hypothesis has been made that yeast RNA Pol I might also be able to be recruited to human rDNA's promoter within the yeast cell and thus transcribe human rDNA.

The goal of project, as shown in (Figure 1. 9), is to build a new model that is able to elucidate RNA Pol I inhibitor with structural explanation based on an elucidated eukaryotic RNA Pol I structure as well as a rDNA template plus promoter, both of which are from Human genome. This model uses yeast cell as the source of RNA Pol I and other necessary transcription factors. The template for rDNA and promoter is from human genome sequence. In this project, human ribosomal DNA (rDNA) plus the promoter was cut out and inserted in yeast integrative plasmid of YIPlac211-TG1 as a generous gift from the lab of Brian C. Rymond. This plasmid contains a sequence of URA3 gene[50] encoding orotidine-5'-phosphate decarboxylase that is an inducing enzyme for synthesis of pyrimidine ribonucleotides de novo[51]. Human rDNA plus promoter is supposed to be integrated within the yeast integrative plasmid containing URA3 gene, of which the expression enables the survival of originally URA3 deficient yeast cells to survive and grow on the medium plate with deficiency in uracil. Therefore, the yeast cells that had successfully incorporated the recombined plasmid containing human rDNA with promoter will be selected. The YBR140C strain of yeast with deficiency in URA3 gene (also a gift from the lab of Brian C. Rymond) was used as the host for selecting the cells with targeted insertion mutagenesis of human rDNA plus promoter following the protocol by Klinner et al (2004)[52]. Thus, a new strain of yeast was created with human rDNA within its genome.

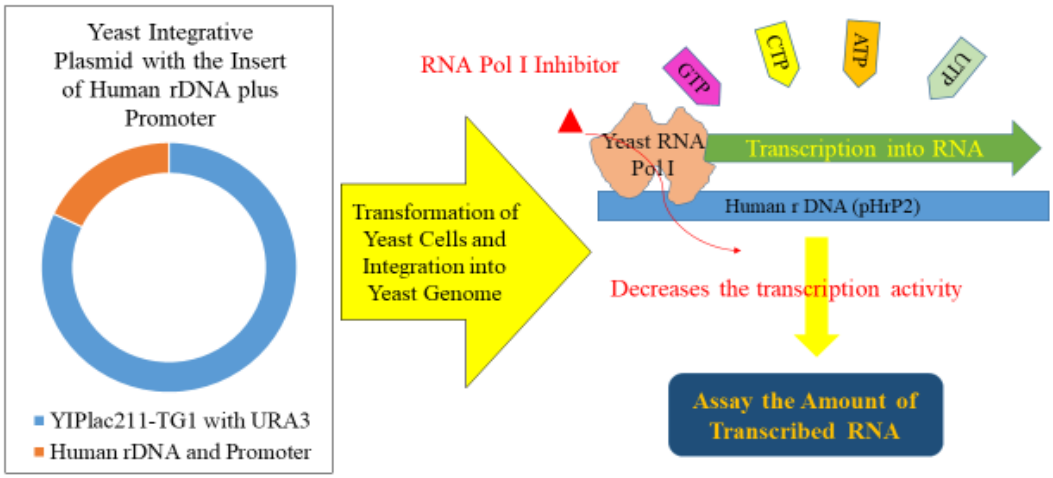

Figure 1.9 Construction of Bio-Model for Assaying Dose Responses of Yeast RNA Pol I to RNA Pol I Inhibitors

Considering the high sensitivity of rDNA to degradation, one strategy of this project is to combine cellular assay of transformed yeast with Human rDNA with quantitative Real Time PCR (qRT-PCR) to quantify the transcription activity of yeast Pol I in transcribing Human rDNA via initiation of the promoter of Human rDNA.

The source of the Human rDNA sequence (plus the promoter) was the plasmid of pHrP2. It was originally made in the lab of Ingrid Grummt and directly from a generous donation from the group of Marikko Laiho at University of John-Hopkins.

CHAPTER 2. EXPERIMENT

2.1 Recombination of Human rDNA and Yeast Integrative Plasmid

The source of the Human rDNA sequence (plus the promoter) was the plasmid of pHrP2, of which the map have been depicted in (Appendix A) and (Appendix C) with respective restriction endonucleases to cut. It was originally made in the lab of Ingrid Grummt and directly from a generous donation from the group of Marikko Laiho at University of John-Hopkins.

At the beginning there were two vector plasmids as template for accepting the insert of human rDNA plus promoter in order to transform the yeast host cells: pRS314-URA3 and YIPlac211-TG1. Both of these vector plasmids contained URA3 gene. Maps of plasmids can be found in the appendix chapter. When the backbone plasmid was pRS314-URA3, the two restriction endonucleases to linearize this template as well as to cut out the insert of human rDNA plus promoter were BamHI-HF and EcoRI-HF as depicted in (Appendix B). When the backbone plasmid was YIPlac211-TG1, the two restriction endonucleases were EcoRI-HF and Hind III-HF as depicted in (Appendix D). The final selection of the two plasmid to make the recombined plamid for the yeast transformation experiment were pHrP2 for the insert and YIPlac211-TG1 for the vector template as briefly depicted in (Figure 2.1). As simplified, the loci of cutting by restriction endonucleases as well as the sizes of the insert and the linearized template were shown in (Figure 2. 1**)**.

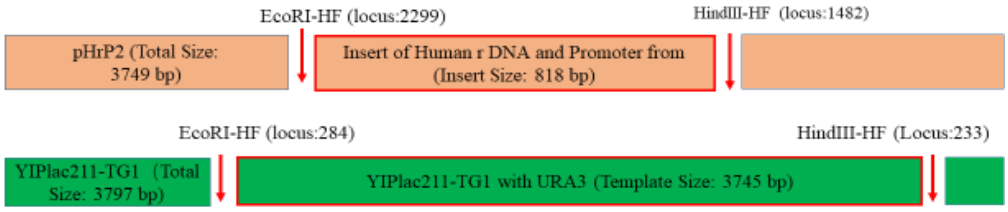

Figure 2.1 Sizes of Target Fragments, Cutting Loci and Restriction Endonucleases for Plasmids

The two plasmids, either pHrP2 for insert or YIPlac211-TG1 for template, was incubated with restriction endonucleases of HindIII-HF and EcoRI-HF together in NEB CutSmart Buffer at 37℃ for 12 hours. Recipes of these two restriction endonuclease reactions were depicted in (Table 2. 1) for pHrP2 and (Table 2.2) for YIPlac211-TG1.

Table 2.1 Recipe of Endonuclease Reactions for pHrP2

Content	Volume
pHrP2 (304.5 ng/μL)	7 μL
HindIII-HF (100 Unit/μL)	1 μL
EcoRI-HF (100 Unit/μL)	2 μL
10 × Cut Smart Buffer	1 μL

Table 2.2 Recipe of Endonuclease Reactions for YIPlac211-TG1

Content	Volume
YIPlac211-TG1 (150.4 ng/μL)	7 μL
HindIII-HF (100 Unit/μL)	1 μL
EcoRI-HF (100 Unit/μL)	2 μL
10 × Cut Smart Buffer	1 μL

The following incubations of the resultant reactions had been run at 65 ℃ for 1 hour. The obtained reaction mixtures were run on agarose gel electrophoresis and the part of agarose gel containing the target bands, either the insert of 818 bps and the template of 3745 base pairs, were cut out under UV light in darkness and the needed DNA segments

were collected using Monarch DNA Gel Extraction Kit from NEB (Catalog #: T1020S, Lot #: 0041607).

For this combination of template and insert, the sequence of insert containing Human rDNA plus promoter was shown in the Appendix Chapter in (Appendix E). The sequence was shown from 5' terminus to 3' terminus that contained human rDNA plus promoter (underscored) and had the sticky ends in bold alphabets. In the restriction endonuclease reactions, the CutSmart buffer from New England Biolab (NEB) was used so that the plasmids could be cut by two endonucleases simultaneously. The insert and the template were ligated using T4 DNA ligase from NEB. In the ligation reaction, the molar ratio of these two segments was controlled to be about HmrDNA: Linearized Backbone Plasmid≈6:1. The incubation was done on a thermocycler at 16℃ for 36 hours for the insert and template to connect at the sticky ends and at 65℃ for 30 minutes so as to inactivate the ligase (Table 2.3). The ligation mixtures containing the recombined plasmids containing the human rDNA inserts were used to transform the chemically competent E. coli 10β cells from NEB in order to amplify the new recombined plasmid of YIPlac211-TG1-HmrDNA. The transformant that had incorporated the recombinant plasmid containing YIPlac211-TG1-HmrDNA plasmid was selected using solid agarose plate of LB medium with 100mg /L of ampicillin sodium salt from Alfa Aesar (Catalog #: J63807; Lot #: M03D004). The survived transformant of E. coli cells in the colonies that grew on the solid plate were amplified in liquid YPD medium at 37℃37liquid YPD medium overnight. Purified plasmid of YIPlac211-TG1-HmrDNA was extracted and purified using a E. Z. N. A. Plasmid DNA Maxi Kit from Omega Bio Tech (Catalog #: D6922-00).

Table 2.3 Recipe for Inserting Human rDNA into YIPlac211-TG1

Content	Volume
Human rDNA from pHrP2 (~99..5 ng/μL)	12 μL
Linearized YIPlac211-TG1 (~105.4 Unit/μL)	2 μL
10 × T4 Ligase Buffer	2 μL
T4 Ligase (2,000 Unit/μL)	1 μL
DEPC Treated Nuclear Free Water	Added to 20 μL

2.2 Transformation of Yeast with Plasmid with Human rDNA

Middle to late log culture of yeast transformant that had an optical density between 2 and 4 was centrifuged to remove the liquid medium. The resulting cell pellet was washed once with sterile DI water and twice with 100 mM of LiAc-TE-EDTA buffer. The resultant yeast cells were finally re-suspended in 2mL of 100 mM LiAc-TE-EDTA buffer. Aliquots of 500μL of the suspended cells was added in 2mL micro centrifuge tubes. A 50 μL of aliquot of 5 mg/mL salmon sperm DNA (heat denatured at 100℃ for 10 minutes) and the plasmid DNA (1 to 3 μg in ≤10 μL) were successively added into and mixed well with the suspended yeast cells. The reaction mixture was incubated at room temperature for 5 minutes and 25 μL of DMSO was added and briefly mixed. After an incubation at room temperature for 30 minutes, the reaction mixture was gently mixed with 2.0 mL of 40% (v: v) PEG 3350 in 100 mM LiAc-TE-EDTA buffer. The reaction mixture was then incubated in a water bath at 30℃ for 30 minutes and heat-shocked at 42℃ for 20 minutes. The yeast cells were spun out and added in 2 mL of YPD broth. The culture was then incubated at 30℃ with shaking at 250 rpm for 1 hour. This outgrowth step is necessary to have sufficient amount of colonies and should always be done. (Once it was not done, there could even be risk that no colony generates.)

The yeast cells were spun out, washed once with 1mL of sterile DI water and spun out again. 1 mL of sterile DI water was added to re-suspend the yeast pellet. All the transformation mixture was plated on the –URA3 selective plate to grow the colonies of the transformant of the yeast.

The introduction of Human rDNA into the yeast cells from the YBR140C strain was verified using PCR as shown in (Figure 2.2**)**. This operation began with a denaturation at 95℃ for 2 minutes followed by a 35-cycle amplification, within which each cycle began with a denaturation for 30 seconds at 95℃, followed by an annealing for 30 seconds at 60 ℃ and finally a sequence extension for 50 seconds at 72 ℃. These amplifying cycles were followed by a 1 round incubation at 72 ℃ for 2 minutes and a final standing incubation at 4 ℃.

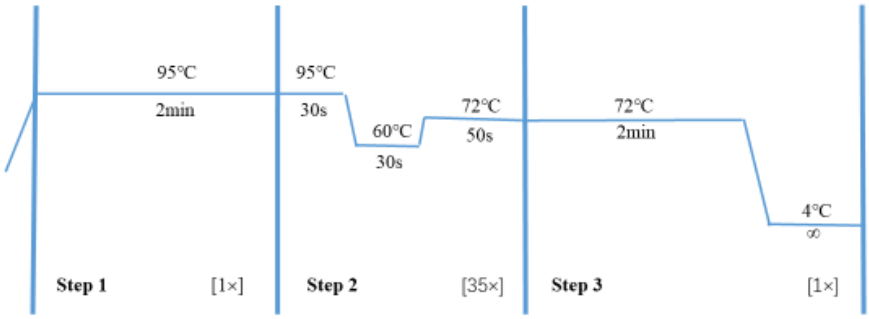

Figure 2.2 PCR Protocol for Detecting Inserted Human rDNA in Total DNA Extract from Strain YBR140C-HmrDNA

2.3 Virtual Screening of NIH/NCATS Library for Possible RNA Pol I Inhibitors

The yeast RNA Polymerase I crystal structure (PDB access number: 5g5l) solved by Engel et al (2016)[16] was downloaded from the Protein Data Bank (https://www.rcsb.org/structure/5g5l). The file of coordinates for the core enzyme structure was obtained using GEDIT by removing the coordinates of the Rrn3 factor.

Using this model, amino acid residues on the surface of A43 subunit within a 2 Å distance from the surface of Rrn3 in the holozyme complex were selected and highlighted. A new Mol2 file was created with the amino acid residues belonging to Rrn3 removed using the program of Autodock PMV-1.5.6. This new PDB file was converted into a mol2 file using the program of Open Babel GUI. This mol2 file of Yeast RNA Pol I was input in the program of SYBYL-X. The biomolecule receptor as the core enzyme part of yeast RNA Pol I was initialized by fixing terminal amino acid residues, removing free water molecules, protonating the biomolecule receptor's atoms and building the hydrogen bonding, assigning Gasteiger charges to the amino acid residues and minimizing the total energy. The multi-channel docking protomol on the structure of Yeast Pol I 5g5l with Rrn3 removed was generated. Pick the docking protomol that included most of the amino acid residues described above.

Using Autodock 1. 5. 6, a region for constructing docking protomol was selected to include and highlight all of the amino acid residues belonging to the interface between RNA Pol I core enzyme and RRN3: PHE138, Ile139, SER141, ALA142, SER143, HIS144, LEU148, ASN154, SER156, LYS158, VAL242, ARG1119, ILE1120, GLY1121 as depicted in (Figure 2.3). The image on the left shows the RNA Pol I core enzyme is in pink and the Rrn3 in green. The three regions in blue are surficial amino acids (which are shown in pink in the box in the image on the right) that have direct contact with Rrn3 in a complex. A docking box including the protomol was generated and depicted in the image on the right side for running the docking of RNA Pol I with possible small molecular compounds as inhibitors. The docking region were confined within the box that is depicted in the box on the right. The grid center coordinates for this

box were x=144.335, y=149.293 and z=99.2 angstroms with numbers of grid points as 126 in x, 40 in y and 126 in z with an interspace of 0.200 angstroms.

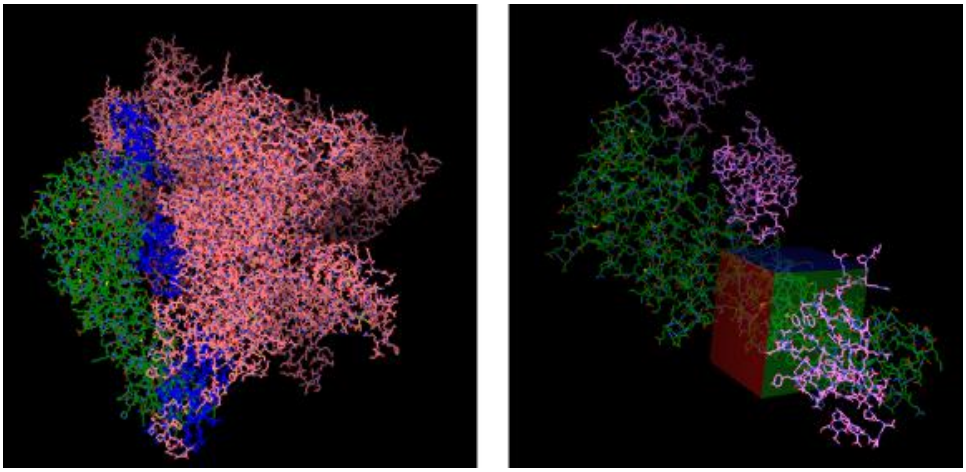

Figure 2.3 Docking Protomol for Screening Yeast RNA Pol I Inhibitors Using Autodock

Multi-channel docking protomols on the structure of yeast Pol I 5g5l were generated and a docking protomol was selected to include the same amino acid residues as included by the box-shaped docking region in the protomol generated by Autodock 1. 5. 6. Virtual structures of 500 compounds from the ZINC/NCATS library were converted into Mol2 format and input into the program of SYBYL-X. RNA Pol I inhibitor screen using SYBYL-X were run using a huge data base including 500 compounds. The docking protomol used for SYBYL-X is depicted in (Figure 2.4**)**. Such a protomol included the surficial regions of crucial Yeast Pol I subunits in rDNA transcription such as RPA43 and RPA190. The compounds were screened with the scores as the negative log values reported. The compounds with the top 5 scores in first round of screening and the top 5 scores in the second round of screening were supposed to be used to run the yeast cellular assays to study their dose dependent effects on the growth. The score was the negative log values of the binding constants regarding the ligands to the protomols within which

they might have contact with the protomol including A43 subunits surface that interacts with Rrn3 and disrupts the binding interaction between this subunit and Rrn3 in order to inhibit the transcription initiation of RNA Pol I.

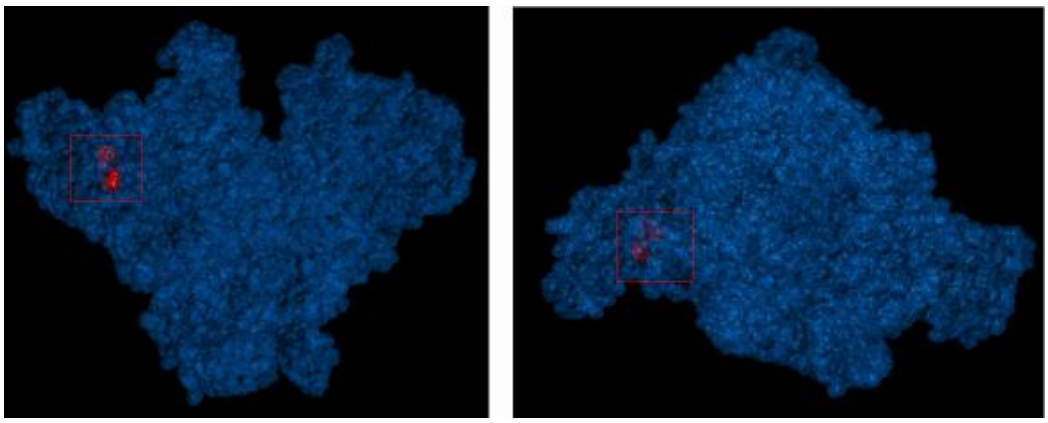

Figure 2.4 Docking Protomol for Screening Small Compounds from ZINC/NCATS Library of 500 Compounds

2.4 Yeast Growth Assay with Ligand Compounds

The following protocol was originally from a published research[53] with our modification. Individual deletion strains arrayed on YPD/agar were inoculated into 100 μL of liquid YPD using a 96-head pin tool. Cultures were grown to saturation overnight at 30 ℃ and then stored at 4 ℃ for 4 hours. The yeast cells were then re-suspended by shaking for 15 minutes and each yeast culture's concentration was normalized by diluting to a final OD_{600} of around 0.02 in a UV fused quartz CV10Q1400S cuvette (Thorlab, Newton, NJ) using a Shimadzu UV-1280 Spectrophotometer (Beckman Coulter. Inc. Altanta, GA). Normalized cultures were grown in 100-μl volumes in 96-well plates in a Tecan GENios microplate reader (MTX Lab Systems, LLC, Bradenton, FL) for 24 h. The growth rate of each culture was monitored by measuring the OD_{570} every 5 min. Each ligand compound was test in the growth assays using not only the yeast cells from the strain of YBR140C transformant with human rDNA but also the yeast cells from wild

type strain of YBR140C that was not transformed. Dose responses of YBR140C-HmrDNA cells growth were tested against Actinomycin D with a series of concentrations of 80μM, 40 μM, 20 μM, 10 μM and 5 μM and against Acebutolol hydrochloride, Aripirazole and Cerivastatin Sodium with a series of concentrations of 50μM, 25 μM, 12.5 μM, 6.25 μM, 3.13 μM and 1.07 μM. The resultant diagrams were plotted using the values of CD_{570} versus the time in minutes.

2.5 Extraction of Yeast Total RNA

Two independent colonies of yeast cells of the YBR140C-HmrDNA strain were incubated using liquid YPD medium at 240 rpm at 33℃ overnight. 1 mL of YPD medium with amplified yeast cells were diluted using fresh liquid YPD medium in a 1: 6 (v: v) ratio. The diluted yeast cells were then shaken at 240 rpm at 33℃ for 6 hours to allow the majority of the amplified cells enter the log phase. For the yeast cells this was done to normalize the transcription activity, which was qualitatively tested by firstly extracting the total RNA and secondly using reverse transcription to generate the corresponding cDNA.

To extract the total RNA, the cells of the transformed yeast strain YBR140C and the wild type YBR140C were both pelleted out into 40μL of final pellets. The pellets were respectively suspended in 100 μL of Yeast Suspension Buffer from the Yeast Total Protein Extraction Kit (GE Health Care, 28-9444-60AA) with 10 μL of Lifelong Zymolyase solutions to lyse the cell walls. The yeast cells were incubate at 37℃ for 1 hour until most of the them became spheroplasts, which were defined as microbes' cells that had the majority of their cell wall removed and were visibly spherical under microscope[54 55]. The total RNA samples of the yeast spheroplasts were extracted using

the OMEGA E. Z. N. A. Bacterial RNA Kit R6950-01. The operation followed the total protocol (file:///D:/Daily%20log%202017-2018/R6950-Bacterial-RNA-Combo-Online-072817.pdf) except that the spheroplasts were lysed by incubation with 350 μL of BRK Lysis Buffer at 4℃ for about 3 hours without vortex with glass beads. The total RNA extract samples were denatured using formamide using the following protocol by Masek et al (2005) [56].

2.6 Transcription of Human rDNA in Yeast by Reverse Transcription

The cDNA of the yeast total RNA was made following the modified typical cDNA Synthesis Protocol of Warm Smart RT×Reverse Transcriptase from New England Biolab Inc (Ipswich, MA). Proper amount of RNA extract sample of yeast was incubated with dNTPs mixture at a final concentration of 0.5 mM, Warm Smart RT×Reverse Transcriptase at a final concentration of 7.5 Unit/mL, Random Primer 6 mixture at a final concentration of 6 μM, 1× Isothermal Amplification Buffer in each reaction mixture with a final volume of 20μL as shown in (Table 2.4). After being mixing by vortexing, all of the reaction mixtures were incubate for 20 minutes at 25℃ for annealing and 60 minutes at 55℃ for synthesis. The reactions were quenched by incubation at 80℃ for 10 minutes in order to inactivate Warm Start RTx Reverse Transcriptase.

The resultant cDNA was then sampled in a PCR with primers that were designed to amplify the human rDNA sequence, the result was visualized using agarose gel electrophoresis to check the possible presence of band corresponding to the size close to 387 base pairs, i. e. the size of the human rDNA.

Table 2.4 Recipe for Reverse Transcription of Yeast Total RNA

Contents	Volume
10 × Isothermal Amplification Buffer	2 μL
10 mM dNTP Mixture	1 μL
Random Primers Mixture (62 μM)	2 μL
Warm Smart RT × Reverse Transcriptase (15,000 Unit/mL)	0.5 μL
RNA Extract Samples	14.5 μL

2.7 Dose Response Test of Human rDNA Transcription to Ligands

Individual aliquot of yeast transformed cells from the strain of YBR140C-HmrDNA arrayed on –URA3 agar were inoculated into 100 μL of liquid YPD medium using a 8-head pin tool. Cultures were grown to saturation over night at 33 ℃ then stored at 4 ℃ for 4 hrs. The cells were then re-suspended by shaking with a vortex to homogenize and the optical density at 600 nm (OD_{600}) of cultures was determined using a Shimadzu UV-1280 Spectrophotometer (Beckman Coulter. Inc, Atlanta, GA). Cell concentrations were normalized by diluting each culture to a final OD_{600} of ~0.02.

Normalized cultures were grown in 100-μl volumes in 96-well plates in Tecan GENios microplate readers for 24 h. The growth rate of each culture was monitored by measuring the OD_{570} every 5 min. Dose responses of YBR140C-HmrDNA cells growth were tested against Cerivastatin Sodium with concentrations of ~1560 nM, 780 nM and 390 nM, 195 nM, and 98 nM; (2) Agatroban with concentrations of ~2500 nM, 1250nM; Aripirazole with concentrations of ~6250 nM, 3125 nM, 1562 nM, 780 nM. The resultant dose response curves were plotted using the values of OD_{570} versus the time in minutes.

The general protocol of running qRT-PCR was derived from the protocol published by Wang et al (2003)[57]. The optimal adhesive covers were from Life Technologies Holdingsp Pte Ltd, Singapore. The MicroAmp Optical 96-Well Reaction

Plates were from Life Technologies Corporation. The PowerUp SYBR Green Master Mix (Universal 2× Master Mix for Real-Time PCR Workflows) was from Thermo Fisher Scientific. The forward and reverse primers for housekeeping genes-MEP2 and PDC1 were both from IDT. The primer mixture targeting the amplicon of Yeast rDNA was from IDT.

The housekeeping gene that was selected to run qRT-PCR was MEP2, the gene encoding an ammonium permease[58]. MEP2 gene encodes an ammonium permease with higher affinity than the counterpart ammonium permeases encoded by MEP1 and MEP3 and is necessary for yeast metabolism[59]. Transcription activities of this enzyme encoding gene was used as reference to normalize the transcription activities of target gene, which was human rDNA plus promoter.

The primers for partially amplifying Human rDNA within the transformed Yeast YBR14C-HmrDNA were the forward primer: 5'-GGGCCTGCTGTTCTCTCG-3' and the reverse primer: 5'-GAGAACGCCTGACACGCA-3'. The size of corresponding amplicon is 197 base pairs with the following sequence in a direction of 5' to 3': GGGCCTGCTGTTCTCTCGCGCGTCCGAGCGTCCCGACTCCCGGTGCCGGCCCG GGTCCGGGTCTCTGACCCACCCGGGGGGCGGCGGGGAAGGCGGCGAGGGCC ACCGTGCCCCCGTGCGCTCTCCGCTGCGGGCGCCCGGGGCGGCCGCGACAAC CCCACCCCGCTGGCTCCGTGCCGTGCGTGTCAGGCGTTCTC. The housekeeping gene that was selected for the RT-PCR was MEP2 gene with the forward primer: 5'-CTGGACATGGTGGTCTAGTT-3' and the reverse primer: 5'-GAGGTGACGGAATGTGGT-3'.

These two primers were used to amplify part of the MEP2 gene's sequence that could yield amplicons of 100 base pairs with the following sequence of CTGGACATGGTGGTCTAGTTTACGCTTTGATACTGGGTAAGCGTAATGACCCT GTTACACGTAAAGGGATGCCCAAGTACAAACCACATTCCGTCACCTC.

Samples without template cDNA as the non-template controls (NTC) were set up with the same dose of SYBR Green master mix with the identical final volumes as the samples with cDNA templates. The recipe of qRT-PCR Reactions for Quantifying Transcription Activity of Yeast RNA Pol I is shown in (Table 2.5). The setups for qRT-PCR were recorded in Appendices from (Appendix F) to (Appendix L).

Table 2.5 Recipe of qRT-PCR for Transcription Activity of Yeast

Component	Volume (20μL/Well)
PowerUP SYBR Green Master Mix (2 ×)	10 μL
Forward and Reverse Primers (4 μM)	3 μL for each
cDNA and Nuclearase-Free Water	~60 ng, 30 ng, 15 ng, 7.5 ng and 3.8 ng for Standard Samples of MEP2 or Human rDNA; ~60 ng for Experimental Samples Amplifying Human rDNA
Total Volume	20 μL

CHAPTER 3. RESULTS AND DISCUSSIONS

3.1 Introducing Human rDNA into Yeast Cells

The first goal of this project was to build a cellular model for studying the transcription of human rDNA by yeast RNA Polymerase I. Choosing YIPlac211-TG1 as template plasmid was more advantageous because its size was smaller than pRS314-URA3. Therefore, YIPlac211-TG1introduces less external DNA sequences into the genome of yeast host. The other reason for making this choice was because the positions of BamHI locus and EcoRI locus within the pRS314-URA3 plasmid was so close (12 base pairs in between) that it seemed difficult to conduct the restriction endonuclease reactions since it took more trials before the insertion was successful. After the first step of plasmid construction, the sequencing result showed the yeast integrative plasmid of YIPlac211-TG1 had successfully incorporated human rDNA plus the promoter from the plasmid of pHrP2 (Figure 3.1).

Agarose gel electrophoresis of linearized YIPlac211-TG1 plasmid as template and human rDNA with promoter as insert. Band 1 in pink box was human rDNA plus promoter that was cut out from the pHrP2 plasmid. This insert sequence has the expected size of ~818 base pairs. Band 2 and Band 3 in green boxes were the linearized YIPlac211-TG1 plasmids with the expected size of ~3745 base pairs. Images from electrophoresis depicted resultant DNA segments from restriction endonuclease reactions. Comparison with bands from a DNA size marker identified the presence of linearized YIPlac211-TG1 plasmid as template as well as an insert composed of human rDNA and its promoter from pHrP2 plasmid (Figure 3.1 A). Comparison between wild type and linearized reconstructive plasmid built after inserting human rDNA with promoter into

the Yeast Integrative plasmid of YIPlac211-TG1. Electrophoresis implicated the size of the new plasmid from reaction of DNA ligase and amplification using E. coli transformation was the same as the expected size of ~3745 base pairs as shown in Lane 4 of (Figure 3.1 B). The general process of cutting out human rDNA plus promoter as insert and linearizing the template plasmid of Yeast Integrative Plasmid YIPlac211-TG1 that contains the same sticky ends as the insert as well as connecting these two parts into a new intact plasmid of YIPlac211-TG1-HmrDNAThe whole process of making Yeast Integrative Plasmid YIPlac211-TG1-HmrDNA was briefly depicted by (Figure 3.1 C).

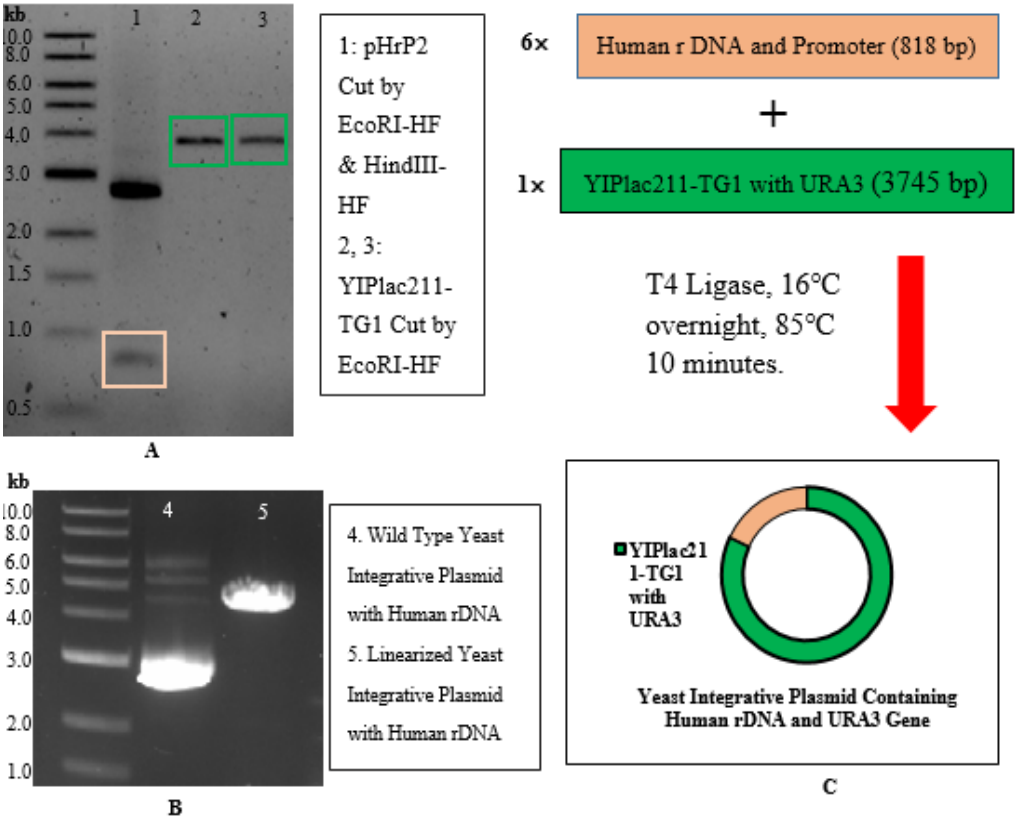

Figure 3.1 Construction of Yeast Integrative Plasmid Containing Human rDNA plus Promoter

In the original plan a reporter gene of firefly luciferase was supposed to be incorporated in the same plasmid adjacent to the 3' end of human rDNA in order to quantify the transcription activity of yeast RNA Pol I in a high throughput activity assay. However, it proved challenging to directly release the reporter luciferase from yeast cell possibly due to the impenetrable yeast cell wall, which is resistant to chemical reagents like DMSO usually used to break the cell membrane of human cells. Meanwhile, degradation of the shield of yeast cell wall requires at least one hour treatment with zymolyase. This process might risk degradation of the expressed luciferase.

Subsequent transformation of YBR140C was done as expected since the sequencing data of the total DNA from the transformed yeast cells showed the presence of human rDNA sequence within the yeast genome. In the transcription test, the total RNA of transformed YBR140C, herein refered to as YBR140C-HmrDNA was reverse-transcribed. To guard against contamination from genomic DNA, the total RNA was treated with DNase. The resultant cDNA was subjected to PCR using primers that can amplify certain sequences of human rDNA followed by agarose gel electrophoresis. Both the presence of the DNA band with the expected sized after amplification and the sequencing result indicated the successful transcription of the human rDNA sequence (Appendix M). These results implicated that yeast RNA Pol I could be recruited to the promoter region of human rDNA to form the transcription initiation complex as well as the elongation complex since the transcription of the incorporated human rDNA had been conducted.

3.2 Identifying the Human rDNA in the Yeast Transformant

The band size close to 378 base pairs for the PCR of the total DNA extracts of YBR140C-HmrDNA Transformant had the close size of the Human rDNA. The result implicated the existence of the Human rDNA within the genome of the YBR140C transformant with the plasmid of YIPlac211-TG1-HmrDNA. The band with a smaller size than 378 base pairs (Figure 3.2) was probably DNA fragments that formed by polynucleotide degradation, which was more obvious for the DNA samples obtained through crude extraction from yeast cells without scrutinized removal or inactivation of cellular Dnase. Lane A shows the result of PCR amplification of total DNA extract of Yeast Strain YBR140C-HmrDNA, which was the strain with inserted sequence of Human rDNA. Lane B was the amplified total DNA extract of Yeast Strain YBR140C-HmrDNA. Lane C was the PCR amplification of pHrP2 Plasmid containing the Human rDNA sequence as a positive control.

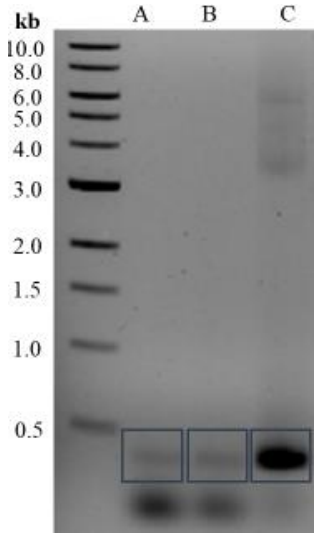

Figure 3.2 Gel Electrophoresis of PCR for Detecting Inserted Human rDNA inYeast Strain of YBR140C-HmrDNA

Sequence alignment of cDNA from yeast transformant of YBR140C-HmrDNA was conducted on the website of Clustal Omega (https://www.ebi.ac.uk/Tools/msa/clustalo/) with the Human rDNA sequence from the sequence map of Plasmid pHrP2. The result (Appendix M) verified the presence of Human rDNA within the cDNA from the reverse transcription of total RNA by the transcription activity of yeast transformant-YBR140C-HmrDNA. The matching percentage between the two sequences that were aligned was 89.3%.

3.3 Virtual Screening of Ligand-RNA Pol I Interaction

Molecular docking study using Autodock 1.5.6 showed that CX-5461 might bind with the protomol on the interface between RNA Pol I core enzyme and RRN3 tightly with a lowest binding free energy of -5.77 k cal/mol. The structure corresponding with such a binding constant was depicted in (Figure 3.3**)**. Molecular docking that followed the same protocol showed that Actinomycin D might bind with the protomol also tightly since its lowest possible binding free energy was -5.88 k cal/mol. The structure corresponding with such a binding constant was depicted in (Figure 3.4**)**.

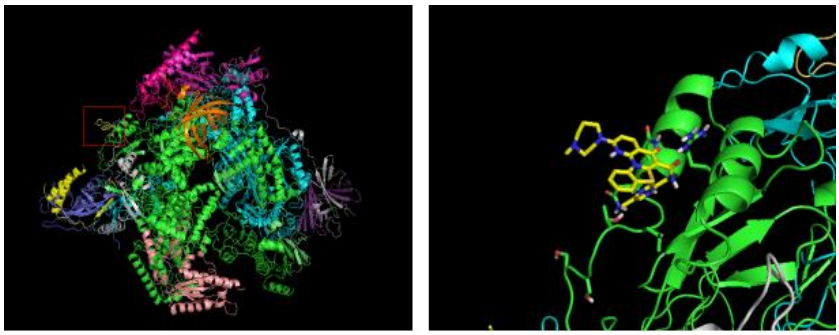

Figure 3.3 Interaction between CX-5461 with Docking Protomol on Yeast RNA Pol I Shown by Autodock

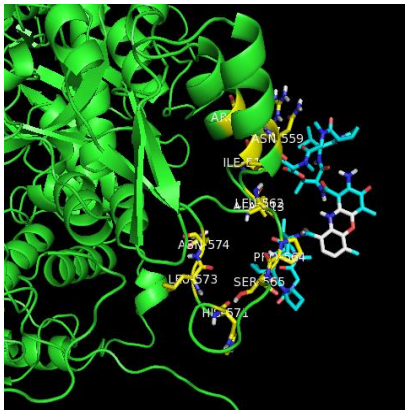

Figure 3.4 Interaction between Actinomycin D with the Surficial Amino Acids that Had Direct Contact with RRN 3 Factor

The same algorithm calculated that cerivastatin sodium had a binding constant of -2.62 k cal/mol. In this docking Arg520, Gln553, Lys555, Asn567 and Glu552 were set as flexible residues, which were intentionally set up in order to make the docking more similar with the real biomolecule within the living yeast cells. The conformation of interacting ligand with the RNA Pol I core enzyme was depicted in (Figure 3. 4).

An ZINC/NCATS small-molecule library of 600 FDA approved compounds were used for the virtual screening. The ligands with the high scores for the first round of screening were selected with a score higher than 10. These were CX-5461 with a total score of 12.0518, Bisoprolol with a total score of 11.4195, Agatroban (NCC-108-04-H04) with a total score of 11.3536, Aripirazole with a score of 10.6326, Cerivastatin Sodium with a score of 10.3224, Telmisartan with a score of 10.3224 as depicted in (Figure 3.5). CX-5461 had already been verified as a strong and selective RNA Pol I inhibitor by prior research, a couple of which were briefly recorded in the introduction section. It was ranked the top most hit and this result seemed to support that this virtual screening strategy could work. Actual dose responses of these screened compounds were still

needed for the ultimate evaluation of these compounds as actual “hits” for designing anticancer drugs.

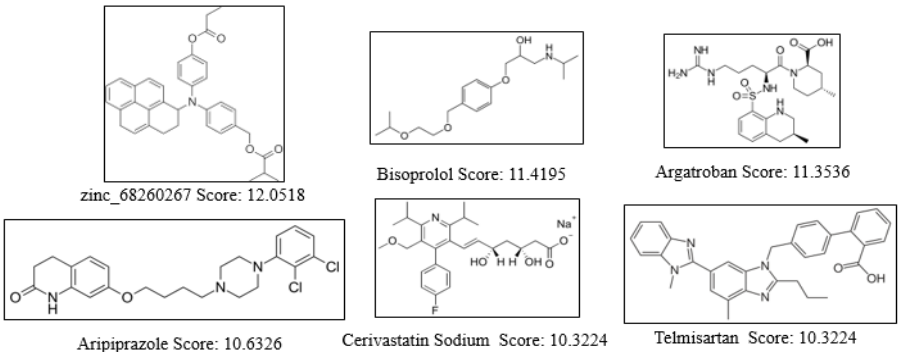

Figure 3.5 Top Six Hits of First Docking Set of 500 ZINC/NCATS Library Compounds with Yeast RNA Pol I

Comparison between the virtual screening result showed that data of CX-5461 from SYBYL-X, with a docking score of 12.0518 and the binding constant of -5.77 k cal/ mol obtained from Autodock were consistent, suggesting that the compound could tightly bind with the protomol on RNA Pol I enzyme in contact with Rrn3. Therefore, the result complied well with the experimentally observed result from prior publications that CX-5461 was a strong inhibitor to RNA Pol I. However, the docking score that was calculated by SYBYL (10.3224) for Cerivastatin Sodium seemed not to comply well with the calculated lowest binding energy as calculated from Autodock 1. 5. 6 (Figure 3.6). This calculated lowest binding energy of Cerivastatin Sodium with RPA43 and RPA190 that interact with Rrn3 was -2.62 k Cal/mol. The possible reason for this inconsistency might be because of different binding affinities between the ligands with the slightly different protomols on RNA Pol I. Further verification using yeast cellular transcription assays of Cerivastatin Sodium with RNA Pol I was therefore necessary.

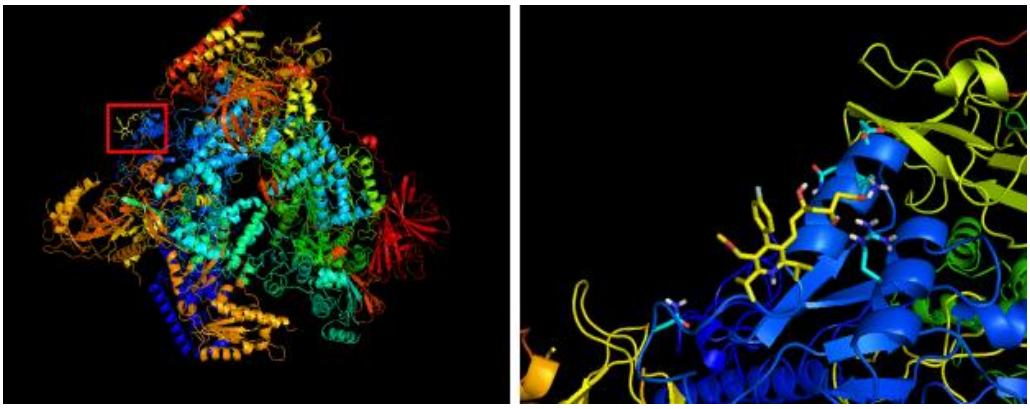

Figure 3.6 Interaction between Cerivastatin Sodium at the Interface with RRN3

Another docking was run with a different protomol composed of interspace between RPA190 and A34.5 and Rrn3 with the same FDA approved ZINC/NCATS Library of 500 compounds were used for the virtual screening following the same protocol. The ligands with the high scores for the first round of screening were also selected with a score higher than 10. These were carvediol (ZINC01530579) with a total score of 10.5365, α-Phylloquinone (ZINC03831330) with a total score of 10.4779, S-Salmeterol (ZINC03799072) with a total score of 10.2004, R-Salmeterol (ZINC03785268) with a total score of 10.1825, Phylloquinone (ZINC12503234) with a total score of 10.1099. These results have been summarized in (Figure 3.7).

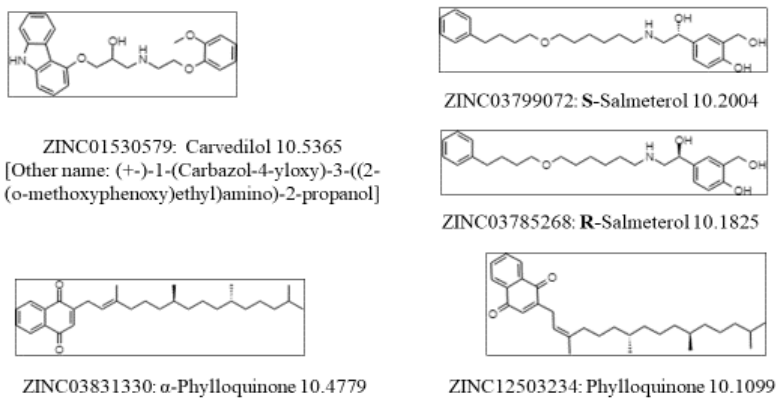

Figure 3.7 Top Five Hits of First Docking Set of Another 500 ZINC Library Compounds with Yeast RNA Pol I

3.4 Identifying the Human rDNA in the Yeast Transformant

The growth of yeast cells was quantified by absorbance versus time at a wavelength of 570 nm. Comparison of absorbance versus concentrations between both wavelengths using samples of yeast cells in liquid YPD media with a series of concentrations diluted in folds of 10 (data not shown). Although originally the absorbance values against time for yeast cell samples with each compound were set up to be for 36 hours, the dynamic ranges were only reported for the portion within 25 hours/1,500 minutes since this length of time was enough to show the yeast samples' dose responses to the ligands to be tested.

Dose dependent responses of a couple of ligands had been conducted to assess their inhibitory effects on the growth of yeast transformant YBR140C-HmrDNA cells. Comparison of the results showed cerivastatin sodium as a stronger inhibitor of growth over actinomycin D. Yeast cells were grown with presence of actinomycin D were conduc with relatively higher concentrations from 80 μM decreasing by two folds to 5 μM (Figure 3.8) and with relatively lower concentrations from 10 μM decreasing to 0.625 μM. (Figure 3.9). Growth assays of yeasts were also set up with concentrations of cerivastatin sodium from 50 μM decreasing to 1.6 μM by two folds (Figure 3.10) and with lower doses of cerivastatin sodium from 1562 nM to 390 μM. (Figure 3.11). Remarkably stronger suppression of yeast growth was observed for incubation with Cerivastatin Sodium in comparison with the diagram depicting yeast growth with presence of Actinomycin D as an established anticancer drug[60] and a transcription inhibitor[61].

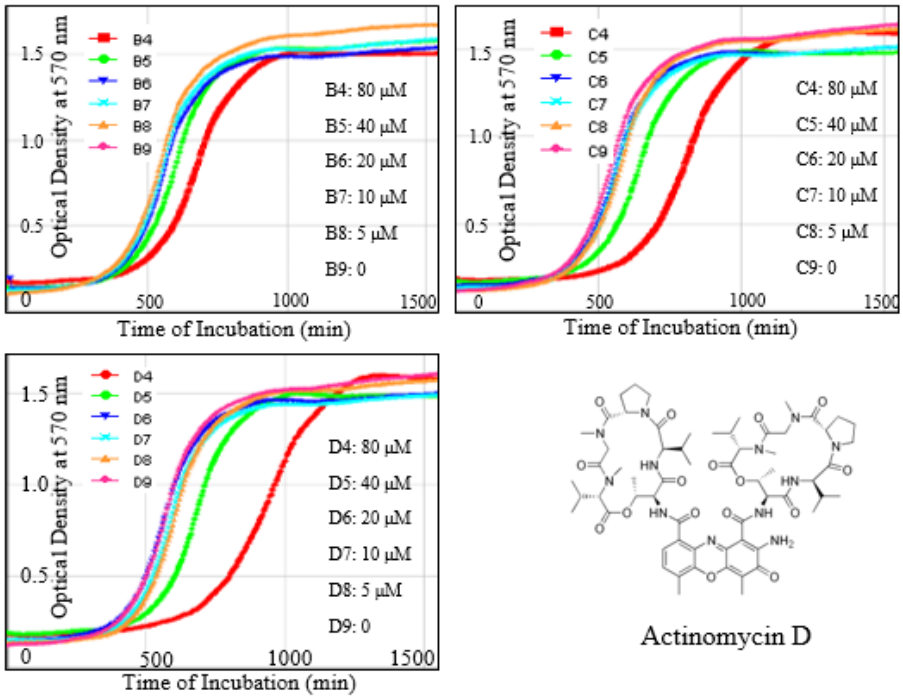

Figure 3.8 Growth Assay of Yeast YBR140C with pHmrDNA-YIPlac211-TG1 with Higher Concentrations of Actinomycin D

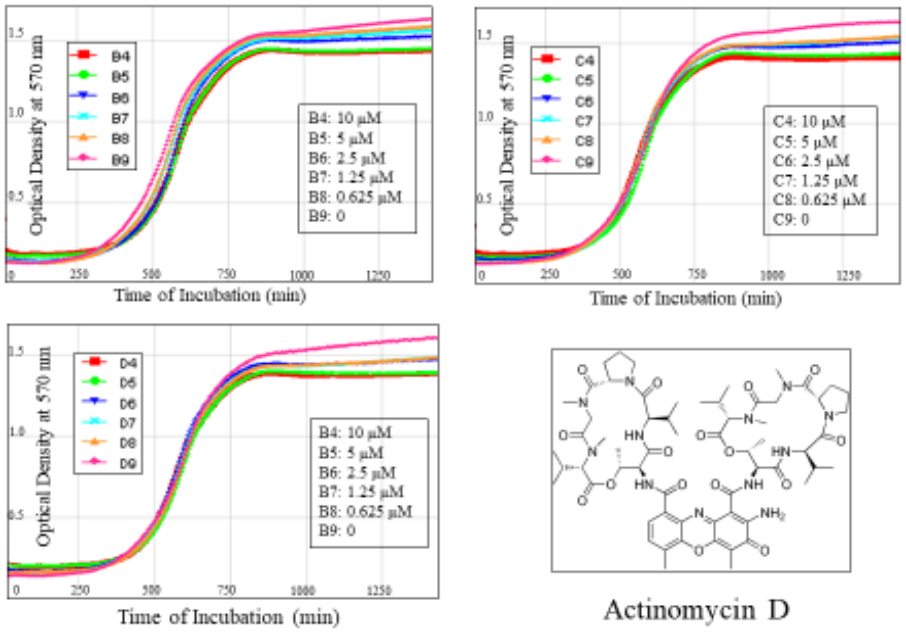

Figure 3.9 Growth Assay of Yeast YBR140C with pHmrDNA-YIPlac211-TG1 with Lower Concentrations of Actinomycin D

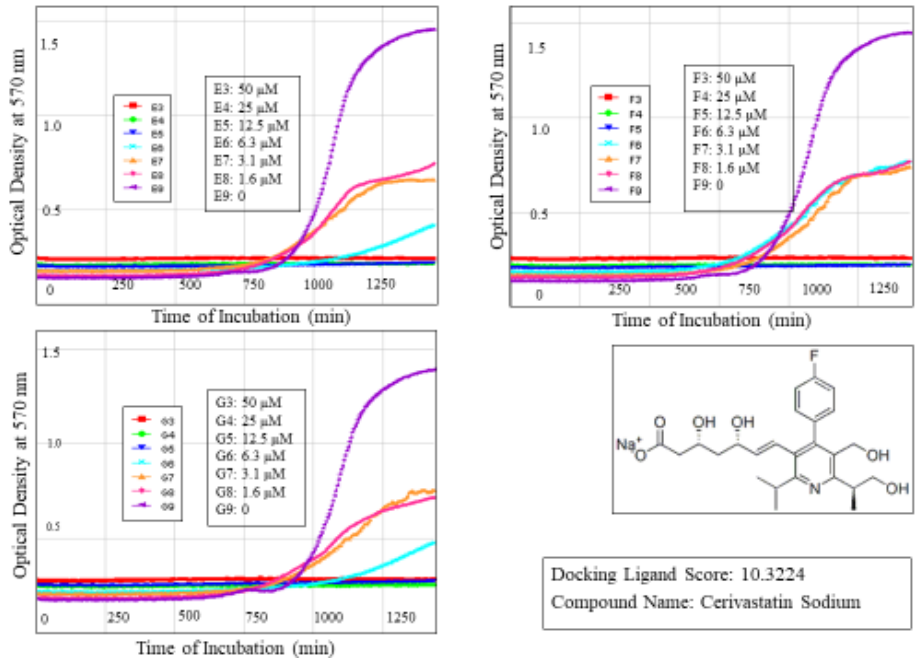

Figure 3.10 Dose Responses of Yeast Growth to Cerivastatin Sodium at Higher Concentrations

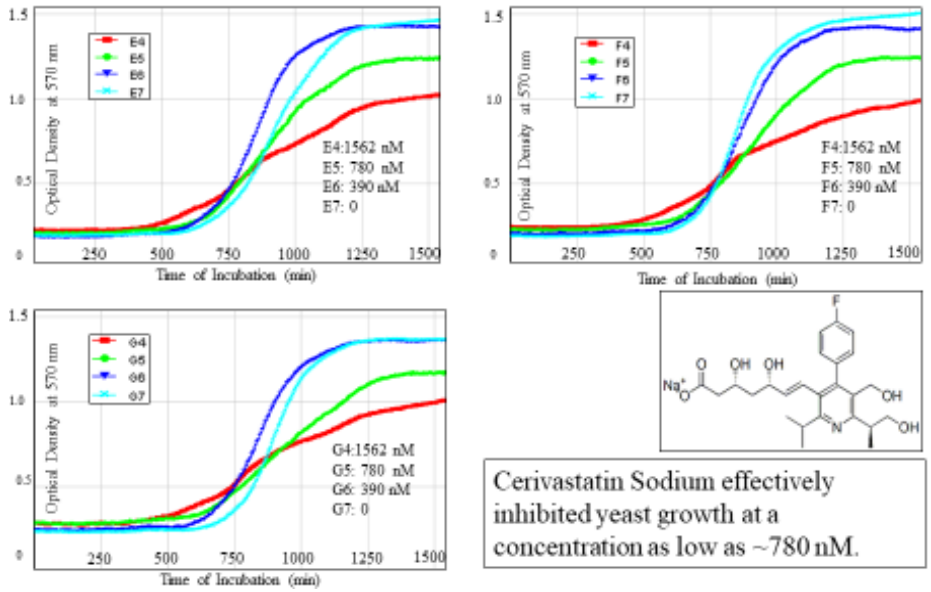

Figure 3.11 Dose Responses of Yeast Growth to Cerivastatin Sodium at Lower Concentrations

Dose response tests of yeast growth to agatroban (Figure 3.12**)** and aripirazole (Figure 3.13) were also shown. Comparison between dose responses implicate that

neither of these compounds were remarkable inhibitors to yeast growth as cerivastatin sodium.

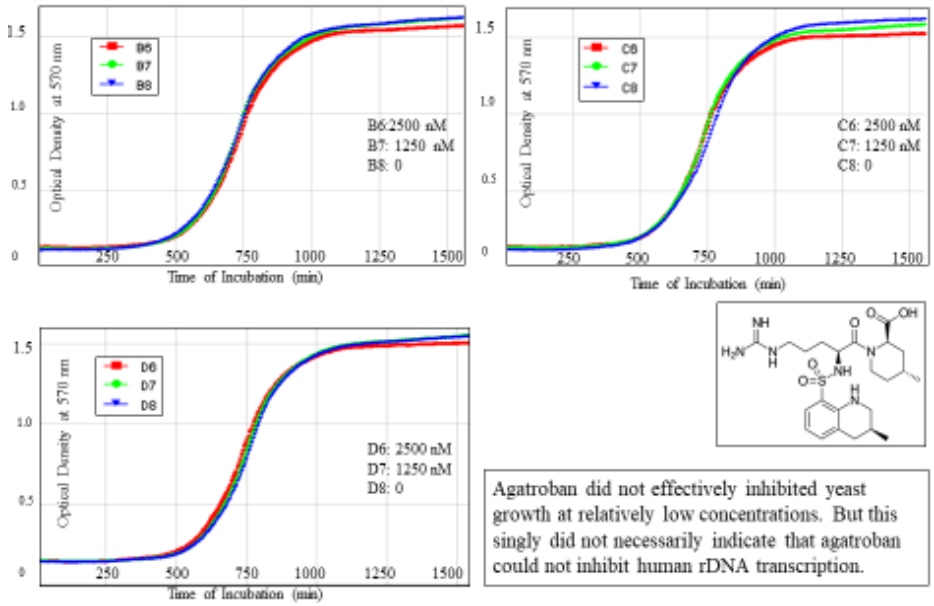

Figure 3.12 Dose Responses of Yeast Growth to Agatroban

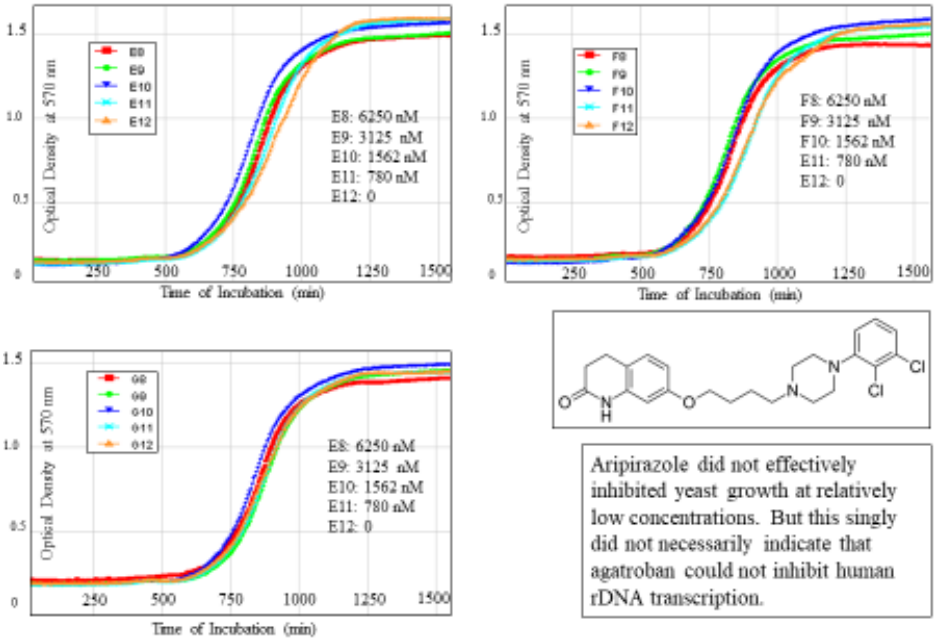

Figure 3.13 Dose Responses of Yeast Growth to Aripirazole

3.5 Dose Response Tests of Human rDNA Transcription by Yeast RNA Pol I

The yeast cells had been successfully transformed and incorporated human rDNA plus promoter and became a new strain of YBR140C-HmrDNA. After the cDNA was obtained from the reverse transcription reaction, its transcription activity was tested using PCR of which the result indicated Human rDNA within the yeast cells was transcribed. Yeast cells that were collected from dose response experiments with a couple of ligands and their cDNA were also extracted and used in reactions of PCR at first and qRT-PCR to test for the possible inhibitory effects on transcription of RNA Pol I.

3.5.1 Detection of Transcription of Human rDNA in Yeast Transformant

The size of the target amplicon was 387 base pairs. As depicted in (Figure 3.14), the band at the end of Lane (a) shows amplicon of the reference plasmid of pHrP2 as the source of human rDNA and promoter. In comparison, amplification reaction of cDNA extracts from yeast transformed strain YBR140C-HmrDNA showed bands with very similar size as depicted in ends of Lane (b) and Lane (c). The reverse transcription test by PCR implicated that the yeast RNA Pol I could transcribe the introduced human rDNA.

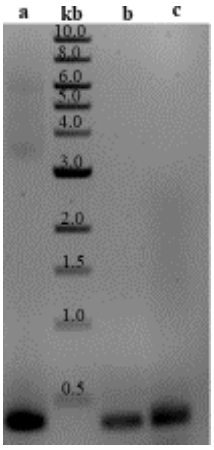

Figure 3.14 Gel Electrophoresis of Amplified 384 bp Human rDNA in Transformed Yeast YBR140C-HmrDNA

The assays were conducted using yeast cells from the transformed strain, YBR140C-HmrDNA. Based on the successful transcription of human rDNA catalyzed by yeast RNA Pol I and the successful reverse transcription, results from PCR amplification of the resultant cDNA were likely to implicate dose dependent inhibition of transcription activity by agatroban and cerivastatin sodium by (Figure 3.15 a) since the density of the target band tended to be increasingly lighter as the dose of ligand decreased. In comparison, a dose dependent inhibition by Aripirazole was not observed (Figure 3.15 b). These observations needed further quantitative assessment as could be done using qRT-PCR.

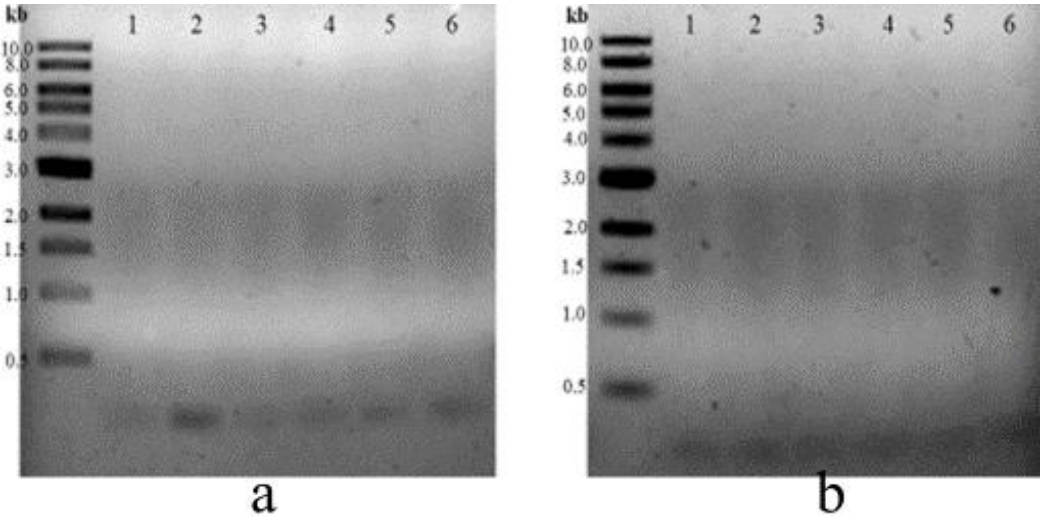

Figure 3.15 Dose Effect of Three Ligands to Transcription of Human rDNA in Yeast. a. Dose response test using Agatroban and Cerivastatin Sodium and ~45 ng of cDNA from YBR140C-HmrDNA. 1: 2500 nM of Agatroban; 2: 1250 nM of Agatroban; 3:1562 nM of Cerivastatin Sodium; 4: 781 nM of Cerivastatin Sodium; 5: 390 nM of Cerivastatin Sodium; 6: without ligand. b. Dose response test using Aripirazole. 1: 6250 nM of Aripirazole; 2: 3125 nM of Aripirazole; 3:1562 nM of Aripirazole; 4: 781 nM of Aripirazole; 5: 3125 nM of Aripirazole; 6: without ligand.

For both cerivastatin sodium and agatroban the PCR products from the transcribed cDNA from the transformed yeast cells of the growth inhibition assay implicated a dose dependent inhibition because as the concentration of ligand increased, the shade of the

band of the PCR amplicon turned out to be increasingly diminished. The results implicated a possible dose dependent inhibitory effect of this compound that might be further verified by experiments in qRT-PCR. In comparison, the effect from Aripirazole on the transcription of human rDNA by Yeast RNA Pol I was not obvious since the densities of the target bands did not show an obvious decreasing tendency as the concentration of Aripirazole increased. Data from qRT-PCR could also lend more evidence to this result.

In the dose dependent inhibition test of small compounds using qRT-PCR, an alternated algorithm that had ever been described by Livak and Schmittgen (2001)[62] was used to derive the target Human rDNA's transcription levels, which were expressed in $2^{-\Delta\Delta CT}$. The C_T values obtained from the results of qRT-PCR reactions, the calculated values from these C_T values and the normalized values of transcription activities were recorded in (Table 3.1**)**. C_T values for house-keeping gene MEP2 and for target Human rDNA were recorded in triplicates of all the three parallel trials that amplifying either target human rDNA or internal control gene of MEP2 for yeast cells incubated with a certain concentration of ligand or without ligand. The differences between C_T values of Human rDNA and MEP2 gene were calculated and recorded as ΔC_T (HmrDNA- MEP2). Their average values were calculated and recorded as ΔC_T[Avg, C_T (HmrDNA)-C_T(MEP2)] with standard deviations. Each ΔC_T [Avg, C_T(HmrDNA)-C_T(MEP2)] value calculated at each concentration of ligand was subtracted by its counterpart ΔC_T[Avg, C_T (HmrDNA)-C_T(MEP2)] value measured in reactions without ligand. The results were recorded as $\Delta\Delta C_T$ [Avg, ΔC_T(with ligand)-Avg, ΔC_T(no ligand)] plus standard deviations. Because of the duplication of DNA during amplification, all of these C_T, ΔC_T and $\Delta\Delta C_T$

values are in logarithm base of 2 and describe the numbers of the amplification cycles of DNA. Relative difference in duplication folds required for specific cDNA to reach the threshold of detection that are in reverse proportion to concentrations of cDNA can thus be calculated using the expression of $2^{-\Delta\Delta CT\ [Avg,\ \Delta CT(with\ ligand)-Avg,\Delta CT(no\ ligand)]}$.

Table 3.1 Summary of Threshold Cycle Values of Threshold Cycles and Normalized cDNA Transcription Activities against Different Ligands with Concentrations by Duplicated Folds

Ligand Concentration	CT Values of HmrDNA			CT Values of MEP2			ΔCT[Avg, CT(HmrDNA)-CT(MEP2)]	ΔΔCT[Avg, ΔCT(with ligand)-Avg,ΔCT(no ligand)]	Normalized Transcription with Ligand to without Ligand, $2^{\Delta\Delta CT}$
No Ligand	30.848	30.937	31.207	23.947	23.672	23.824	7.18±0.25	0.00±0.25	1.00 (0.84-1.19)
390 nM Cerivastatin Sodium	31.380	30.798	30.628	22.862	22.772	22.972	8.07±0.43	0.88±0.43	0.54 (0.40-0.73)
780 nM Cerivastatin Sodium	31.393	31.574	31.275	22.360	22.400	22.447	9.01±0.17	1.83±0.17	0.28 (0.25-0.317)
1562 nM Cerivastatin Sodium	31.791	31.999	32.363	23.665	23.714	23.447	8.44±0.42	1.26±0.42	0.42 (0.31-0.56)
1250 nM Agatroban	31.243	32.631	31.326	24.357	24.340	24.216	7.43±0.76	0.25±0.76	0.84 (0.50-1.42)
2500 nM Agatroban	31.316	31.439	31.596	22.800	22.690	22.750	8.70±0.17	1.52±0.17	0.35 (0.31-0.39)
780 nM Aripirzole	31.278	31.285	31.872	23.947	23.672	23.824	7.66±0.36	0.48±0.36	0.72 (0.56-0.92)
1562 nM Aripirazole	31.180	31.808	31.129	24.201	24.467	26.358	6.36±1.39	-0.82±1.39	1.76 (0.67-4.63)
3125 nM Aripirazole	32.141	31.679	32.137	24.995	25.552	25.644	6.59±0.52	-0.59±0.52	1.5 (1.06-2.16)
6250 nM Aripirazole	31.516	32.821	32.176	24.263	23.829	24.517	7.97±0.91	0.78±0.91	0.58 (0.31-1.09)

These normalized transcription activity values with standard deviations were plotted against three ligands with concentrations increasing with duplicating folds as depicted in Figure (Figure 3.16). These reactions showed that both agatroban and cerivastatin sodium could inhibit the transcription activity of yeast RNA Pol I by measuring human rDNA levels in a dose-dependent manner. Cerivastatin sodium seemed to be a stronger RNA Pol I inhibitor since a decrease by ~46% in transcription activity was observed for the yeast Pol I reaction with a ligand concentration of 390 nM. At higher duplicated concentrations of 780 nM and 1562 nM the inhibitory effects increased as the corresponding transcription activities decreased by ~72% and ~58%. Of these the seemingly stronger decrease in transcription activity with a lower ligand

concentration was probably due to experimental errors accompanied with the handling of decreased yeast cell densities in the liquid medium that could be retrieved in (Figure 3.16). In comparison Agatroban also reduced activities of RNA Pol I by ~16% and ~65% at both concentrations of 2500 nM and 1250 nM. But a lower concentration of Cerivastatin Sodium turned out to be a stronger inhibitor of transcription activity of Human rDNA than Agatroban in that RNA Pol I activity only had about half of its original activity with presence of 390 nM of cerivastatin sodium whereas yeast RNA Pol I still had ~84% of activity when the concentration of Agatroban had already reached 1250 nM, which was 860 nM higher than the concentration of cerivastatin sodium. Inhibition of transcription inhibition of Human rDNA by aripirazole still needed reproducible results from qRT-PCR experiment. There was an unusual increase of normalized transcription activity and standard deviations for compounds treated with aripirazole. However, since a relatively low concentration of aripirazole at 780 nM caused decrease in transcription activity, this compound might still be a potential inhibitor of RNA Pol I's transcription activity. A more rigorous biological evaluation is required.

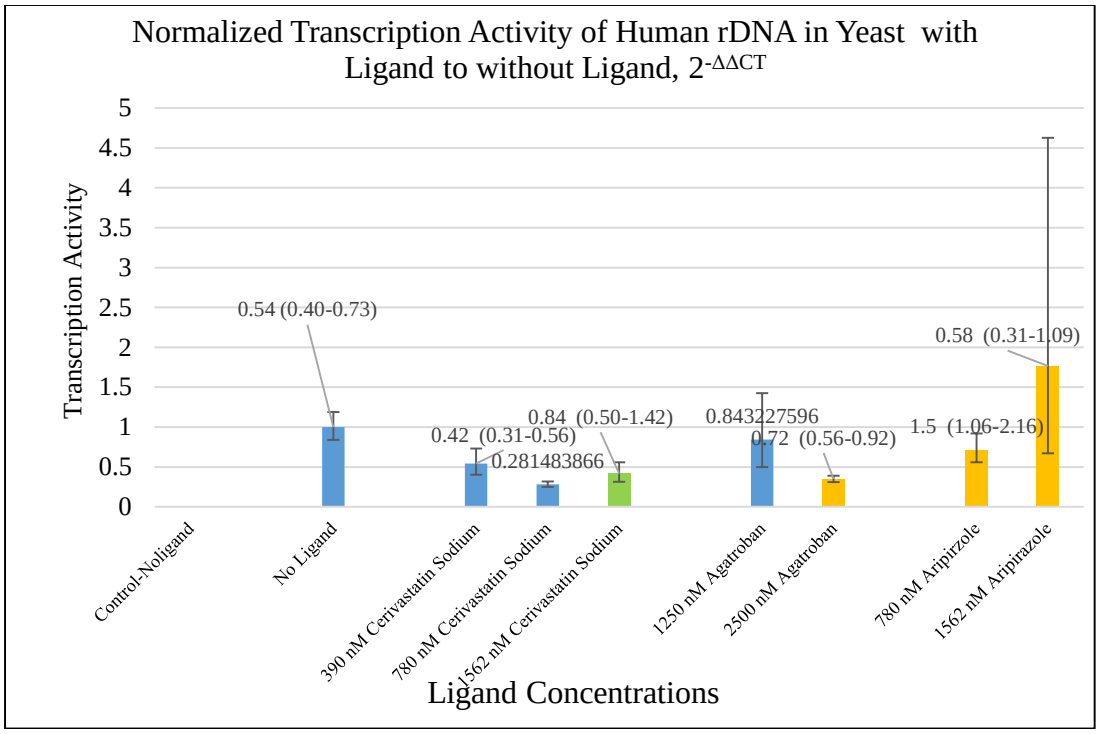

Figure 3.16 Dose Effects of Ligands to Transcription of Human rDNA in Yeast

CHAPTER 4. CONCLUSION

An assay for quantifying transcription activities of RNA Polymerase I has been developed. We successfully verified that yeast RNA Pol I could transcribe the incorporated human's rDNA. This observation strongly implicated a transcription complex had formed by the transcription factors of our transformed yeast cells. It is possible that yeast RNA Pol I was recruited to the human promoter sequence that had been incorporated into our yeast cells. More direct data for this recruitment are needed as a more compelling evidence. To start with, experiments can be designed to find out evidence for DNA-protein interaction between Yeast RNA Pol I and promoter of human rDNA using electrophoretic mobility shift assay (EMSA)[63]. This experiment requires both purified RNA Polymerase together with the transcription factors like RRN3, SL1 as well as a DNA sequence containing human rDNA promoter. In addition, the experiment requires a gel electrophoresis with two comparison groups using the yeast cDNA containing sequences of human rDNA plus its promoter region with or without an incubation with the yeast cell nuclear extract that contains RNA Pol I. The electrophoretic image for the reaction with absence of the band corresponding to the amplicons of human rDNA plus the promoter sequence would implicate the binding of RNA Pol I because the amplicons of this reaction could not move since they are in complex with RNA Pol I.

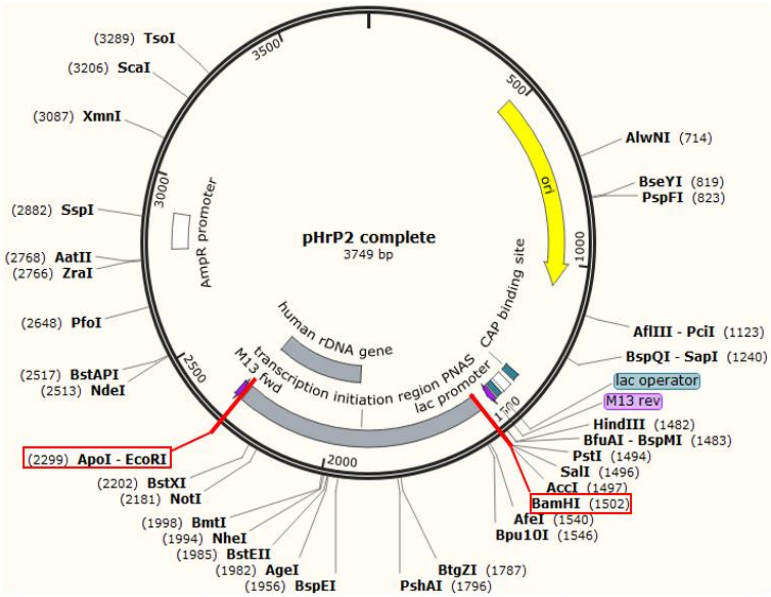

Appendix A Plasmid Maps of pHrP2 that Was Cut by Restriction Endonucleases EcoRI and BamHI

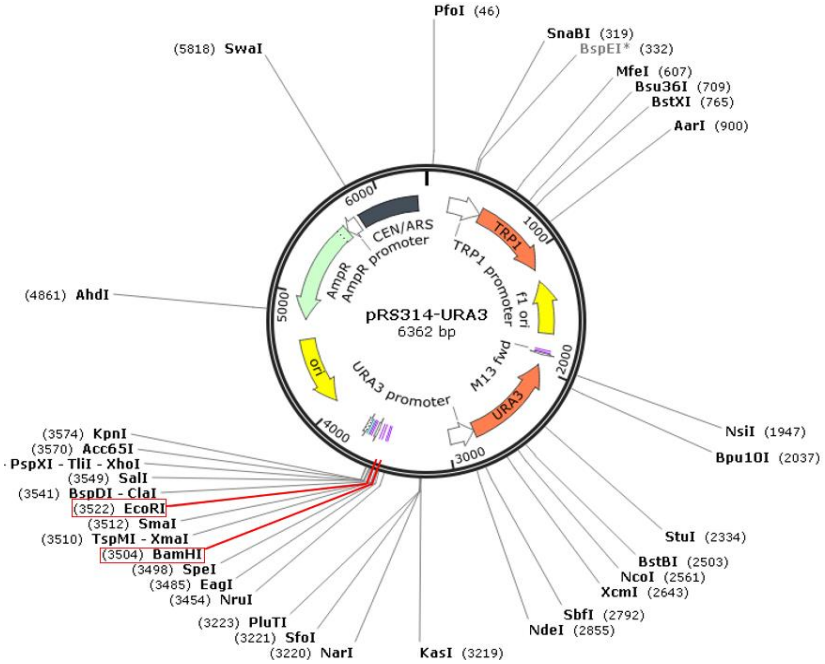

Appendix B Plasmid Map of pRS314-URA3 that Was Cut by Restriction Endonucleases EcoRI and BamHI

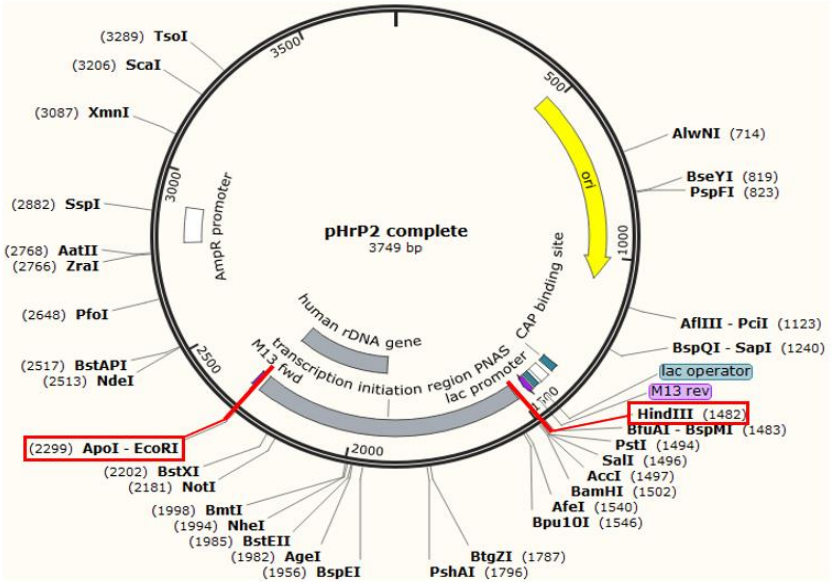

Appendix C Plasmid Maps of pHrP2 that Was Cut by Restriction Endonucleases EcoRI and HindIII

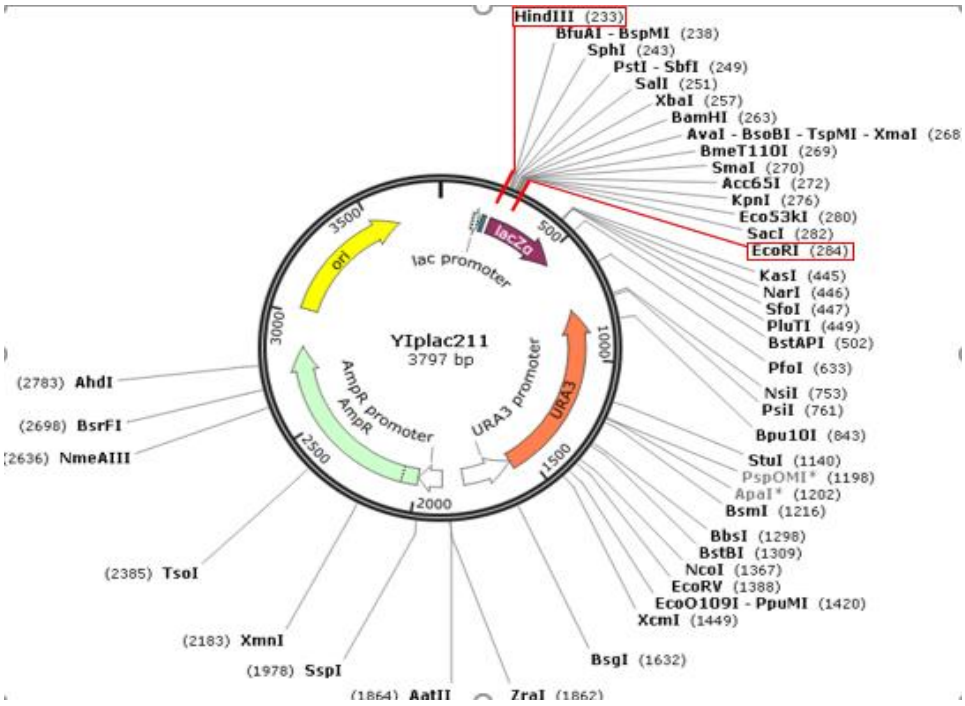

Appendix D Plasmid Map of YIPlac211-TG-1 that Was Cut by Restriction Endonucleases EcoRI and HindIII

AAGCTTGGCTGCAGGTCGACGGATCCTTTCTGGCGAGTCCCCGTGCGGA
GTCGGAGAGCGCTCCCTGAGCGCGCGTGCGGCCCGAGAGGTCGCGCCTG
GCCGGCCTTCGGTCCCTCGTGTGTCCCGGTCGTAGGAGGGGCCGGCCGA
AAATGCTTCCGGCTCCCGCTCTGGAGACACGGGCCGGCCCCCTGCGTGT
GGCACGGGCGGCCGGGAGGGCGTCCCCGGCCCGGCGCTGCTCCCGCGT
GTGTCCTGGGGTTGACCAGAGGGCCCCGGGCGCTCCGTGTGTGGCTGCG
ATGGTGGCGTTTTTGGGGACAGGTGTCCGTGTCGCGCGTCGCCTGGGCC
GGCGGCGTGGTCGGTGACGCGACCTCCCGGCCCCGGGGGAGGTATATCT
TTCGCTCCGAGTCGGCATTTTGGGCCGCCGGGTTATTGCTGACACGCTGT
CCTCTGGCGACCTGTCGCTGGAGAGGTTGGGCCTCCGGATGCGCGCGGG
GCTCTGGCCTACCGGTGACCCGGCTAGCCGGCCGCGCTCCTGCTTGAGC
CGCCTGCCGGGGCCCGCGGGCCTGCTGTTCTCTCGCGCGTCCGAGCGTC
CCGACTCCCGGTGCCGGCCCGGGTCCGGGTCTCTGACCCACCCGGGGGG
CGGCGGGGAAGGCGGCGAGGGCCACCGTGCCCCCGTGCGCTCTCCGCTG
CGGGCGCCCGGGGCGGCCGCGACAACCCCACCCCGCTGGCTCCGTGCCG
TGCGTGTCAGGCGTTCTCGTCTCCGCGGGGTTGTCCGCCGCCCCTTCCCC
GGAGTGGGGGGTTGGCCGGAGCCGATCCCCGG**GAATTC**

Appendix E Sequence of Insert Containing Human rDNA Plus Promoter that Were Integrated within the Yeast Integrative Plasmid of YIPlac211-TG1

Appendix F Setup of Non-Template Control Samples for RT-PCR of Dose Response Tests of Small Compounds to RNA Pol I with Primers for Human rDNA

Well Number	Content	SYBR Green (2×)	Yeast HmrDNA Primer Mix_RT-PCR (4μM)	DEPC Water
1A	NTC for HmrDNA	10 μL	3μL	7μL
1B	NTC for HmrDNA	10 μL	3 μL	7 μL

Appendix G Setup of Non-Template Control Samples for RT-PCR of Dose Response Tests of Small Compounds to RNA Pol I with Primers for House-Keeping MEP Gene

Well Number	Content	SYBR Green (2×)	MEP2 FWD (4μM)	MEP2 REV (4μM)	DEPC Water
1C	NTC for HmrDNA	10 μL	3 μL	3 μL	4 μL
1D	NTC for HmrDNA	10 μL	3 μL	3 μL	4 μL

Appendix H Setup of Standard House Keeping MEP2 Gene's Amplification in qRT-PCR with Two-Fold Dilutions from 60 ng/Reaction

Well Number	Content	SYBR Green(2×)	MEP2 FWD (4μM)	MEP2 REV (4μM)	cDNA
1 E	Standard cDNA 1× MEP2	10 μL	3μL	3μL	4 μL of ~15 ng/μL
1 F	Standard cDNA 1× MEP2	10 μL	3μL	3μL	4 μL of ~15 ng/μL
1 G	Standard cDNA 1× MEP2	10 μL	3μL	3μL	4 μL of ~15 ng/μL
1 H	Standard cDNA1/2 MEP2	10 μL	3μL	3μL	4 μL of ~7.5 ng/μL
2 A	Standard cDNA1/2 MEP2	10 μL	3μL	3μL	4 μL of ~7.5 ng/μL
2 B	Standard cDNA1/2 MEP2	10 μL	3μL	3μL	4 μL of ~7.5 ng/μL
2 C	Standard cDNA1/4 MEP2	10 μL	3μL	3μL	4 μL of ~3.8 ng/μL
2 D	Standard cDNA1/4 MEP2	10 μL	3μL	3μL	4 μL of ~3.8 ng/μL
2 E	Standard cDNA1/4 MEP2	10 μL	3μL	3μL	4 μL of ~3.8 ng/μL
2 F	Standard cDNA1/8 MEP2	10 μL	3μL	3μL	4 μL of ~1.9 ng/μL
2 G	Standard cDNA1/8 MEP2	10 μL	3μL	3μL	4 μL of ~1.9 ng/μL
2 H	Standard cDNA1/8 MEP2	10 μL	3μL	3μL	4 μL of ~1.9 ng/μL
3 A	Standard cDNA1/16 MEP2	10 μL	3μL	3μL	4 μL of ~0.95 ng/μL
3 B	Standard cDNA1/16 MEP2	10 μL	3μL	3μL	4 μL of ~0.95 ng/μL
3 C	Standard cDNA1/16 MEP2	10 μL	3μL	3μL	4 μL of ~0.95 ng/μL

Appendix I Setup of Standard Human rDNA's Amplification in qRT-PCR with Two-Fold Dilutions from 60 ng/Reaction

Well Number	Content	SYBR Green (2×)	FWD and REV Primer Mix of HmrDNA (4μM)	DEPC Water (4μM)	cDNA
3 D	Standard cDNA 1× HmrDNA	10 μL	3μL	3μL	4 μL of ~15 ng/μL
3 E	Standard cDNA 1× HmrDNA	10 μL	3μL	3μL	4 μL of ~15 ng/μL
3 F	Standard cDNA 1× HmrDNA	10 μL	3μL	3μL	4 μL of ~15 ng/μL
3 G	Standard cDNA1/2 HmrDNA	10 μL	3μL	3μL	4 μL of ~7.5 ng/μL
3 H	Standard cDNA1/2 HmrDNA	10 μL	3μL	3μL	4 μL of ~7.5 ng/μL
4 A	Standard cDNA1/2 HmrDNA	10 μL	3μL	3μL	4 μL of ~7.5 ng/μL
4 B	Standard cDNA1/4 HmrDNA	10 μL	3μL	3μL	4 μL of ~3.8 ng/μL
4 C	Standard cDNA1/4 HmrDNA	10 μL	3μL	3μL	4 μL of ~3.8 ng/μL
4 D	Standard cDNA1/4 HmrDNA	10 μL	3μL	3μL	4 μL of ~3.8 ng/μL
4 E	Standard cDNA1/8 HmrDNA	10 μL	3μL	3μL	4 μL of ~1.9 ng/μL
4 F	Standard cDNA1/8 HmrDNA	10 μL	3μL	3μL	4 μL of ~1.9 ng/μL
4 G	Standard cDNA1/8 HmrDNA	10 μL	3μL	3μL	4 μL of ~1.9 ng/μL
4 H	Standard cDNA1/16 HmrDNA	10 μL	3μL	3μL	4 μL of ~0.95 ng/μL
5 A	Standard cDNA1/16 HmrDNA	10 μL	3μL	3μL	4 μL of ~0.95 ng/μL
5 B	Standard cDNA1/16 HmrDNA	10 μL	3μL	3μL	4 μL of ~0.95 ng/μL

Appendix J Setup of Human rDNA's Dose Response Using qRT-PCR to Ligands of Agatroban, Cerivastatin Sodium and Aripirazole

Well Number	Content	SYBR Green (2×)	Primer Mix for Amplifying HmrDNA (4μM)	cDNA	DEPC Water
5 C	Sample 2500 nMAgatroban	10 μL	3μL	4 μLof ~15 ng/μL	3μL
5 D	Sample 2500 nM Agatroban	10 μL	3μL	4 μL of ~15 ng/μL	3μL
5 E	Sample 2500 nM Agatroban	10 μL	3μL	4 μL of ~15 ng/μL	3μL
5 F	Sample 1250 nM Agatroban	10 μL	3μL	4 μLof ~15 ng/μL	3μL
5 G	Sample 1250 nM Agatroban	10 μL	3μL	4 μL of ~15 ng/μL	3μL
5 H	Sample 1250 nM Agatroban	10 μL	3μL	4 μL of ~15 ng/μL	3μL
6 A	Sample 1562 nM Cerivastatin Sodium	10 μL	3μL	4 μLof ~15 ng/μL	3μL
6 B	Sample 1562 nM Cerivastatin Sodium	10 μL	3μL	4 μL of ~15 ng/μL	3μL
6 C	Sample 1562 nM Cerivastatin Sodium	10 μL	3μL	4 μL of ~15 ng/μL	3μL
6 D	Sample 780 nM Cerivastatin Sodium	10 μL	3μL	4 μLof ~15 ng/μL	3μL
6 E	Sample 780 nM Cerivastatin Sodium	10 μL	3μL	4 μL of ~15 ng/μL	3μL
6 F	Sample 780 nM Cerivastatin Sodium	10 μL	3μL	4 μL of ~15 ng/μL	3μL
6 G	Sample 390 nM Cerivastatin Sodium	10 μL	3μL	4 μLof ~15 ng/μL	3μL
6 H	Sample 390 nM Cerivastatin Sodium	10 μL	3μL	4 μL of ~15 ng/μL	3μL
7 A	Sample 390 nM Cerivastatin Sodium	10 μL	3μL	4 μL of ~15 ng/μL	3μL
7 B	Sample 6250 nM Aripirazole	10 μL	3μL	4 μLof ~15 ng/μL	3μL
7 C	Sample 6250 nM Aripirazole	10 μL	3μL	4 μL of ~15 ng/μL	3μL
7 D	Sample 6250 nM Aripirazole	10 μL	3μL	4 μL of ~15 ng/μL	3μL
7 E	Sample 3125 nM Aripirazole	10 μL	3μL	4 μLof ~15 ng/μL	3μL
7 F	Sample 3125 nM Aripirazole	10 μL	3μL	4 μL of ~15 ng/μL	3μL
7 G	Sample 3125 nM Aripirazole	10 μL	3μL	4 μL of ~15 ng/μL	3μL
7 H	Sample 1562 nM Aripirazole	10 μL	3μL	4 μLof ~15 ng/μL	3μL
8 A	Sample 1562 nM Aripirazole	10 μL	3μL	4 μL of ~15 ng/μL	3μL
8 B	Sample 1562 nM Aripirazole	10 μL	3μL	4 μL of ~15 ng/μL	3μL
8 C	Sample 780 nM Aripirazole	10 μL	3μL	4 μLof ~15 ng/μL	3μL
8 D	Sample 780 nM Aripirazole	10 μL	3μL	4 μL of ~15 ng/μL	3μL
8 E	Sample 780 nM Aripirazole	10 μL	3μL	4 μL of ~15 ng/μL	3μL
8 F	Sample without Ligand	10 μL	3μL	4 μLof ~15 ng/μL	3μL
8 G	Sample without Ligand	10 μL	3μL	4 μL of ~15 ng/μL	3μL
8 H	Sample without Ligand	10 μL	3μL	4 μL of ~15 ng/μL	3μL

Appendix K Setup of House-Keeping MEP2 Gene's Dose Response to Agatroban, Cerivastatin Sodium and Aripirazole in qRT-PCR

Well Number	Ligand that was incubated with Yeast YBR140C-HmrDNA for cDNA	SYBR Green (2×)	MEP2 FWD (4μM)	MEP2 REV (4μM)	cDNA of Yeast with Different Doses of Ligands or without Ligand
9A	Sample 2500 nMAgatroban	10 μL	3μL	3μL	4 μLof ~15 ng/μL
9B	Sample 2500 nM Agatroban	10 μL	3μL	3μL	4 μLof ~15 ng/μL
9C	Sample 2500 nM Agatroban	10 μL	3μL	3μL	4 μLof ~15 ng/μL
9D	Sample 1250 nM Agatroban	10 μL	3μL	3μL	4 μLof ~15 ng/μL
9E	Sample 1250 nM Agatroban	10 μL	3μL	3μL	4 μLof ~15 ng/μL
9F	Sample 1250 nM Agatroban	10 μL	3μL	3μL	4 μLof ~15 ng/μL
9G	Sample 1562 nM Cerivastatin Sodium	10 μL	3μL	3μL	4 μLof ~15 ng/μL
9H	Sample 1562 nM Cerivastatin Sodium	10 μL	3μL	3μL	4 μLof ~15 ng/μL
10A	Sample 1562 nM Cerivastatin Sodium	10 μL	3μL	3μL	4 μLof ~15 ng/μL
10B	Sample 780 nM Cerivastatin Sodium	10 μL	3μL	3μL	4 μLof ~15 ng/μL
10C	Sample 780 nM Cerivastatin Sodium	10 μL	3μL	3μL	4 μLof ~15 ng/μL
10D	Sample 780 nM Cerivastatin Sodium	10 μL	3μL	3μL	4 μLof ~15 ng/μL
10E	Sample 390 nM Cerivastatin Sodium	10 μL	3μL	3μL	4 μLof ~15 ng/μL
10F	Sample 390 nM Cerivastatin Sodium	10 μL	3μL	3μL	4 μLof ~15 ng/μL
10G	Sample 390 nM Cerivastatin Sodium	10 μL	3μL	3μL	4 μLof ~15 ng/μL
10H	Sample 6250 nM Aripirazole	10 μL	3μL	3μL	4 μLof ~15 ng/μL
11A	Sample 6250 nM Aripirazole	10 μL	3μL	3μL	4 μLof ~15 ng/μL
11B	Sample 6250 nM Aripirazole	10 μL	3μL	3μL	4 μLof ~15 ng/μL
11C	Sample 3125 nM Aripirazole	10 μL	3μL	3μL	4 μLof ~15 ng/μL
11D	Sample 3125 nM Aripirazole	10 μL	3μL	3μL	4 μLof ~15 ng/μL
11E	Sample 3125 nM Aripirazole	10 μL	3μL	3μL	4 μLof ~15 ng/μL
11F	Sample 1562 nM Aripirazole	10 μL	3μL	3μL	4 μLof ~15 ng/μL
11G	Sample 1562 nM Aripirazole	10 μL	3μL	3μL	4 μLof ~15 ng/μL
11H	Sample 1562 nM Aripirazole	10 μL	3μL	3μL	4 μLof ~15 ng/μL
12A	Sample 780 nM Aripirazole	10 μL	3μL	3μL	4 μLof ~15 ng/μL
12B	Sample 780 nM Aripirazole	10 μL	3μL	3μL	4 μLof ~15 ng/μL
12C	Sample 780 nM Aripirazole	10 μL	3μL	3μL	4 μLof ~15 ng/μL
12D	Sample No Ligand	10 μL	3μL	3μL	4 μLof ~15 ng/μL
12E	Sample No Ligand	10 μL	3μL	3μL	4 μLof ~15 ng/μL
12F	Sample No Ligand	10 μL	3μL	3μL	4 μLof ~15 ng/μL

Appendix L Layout of Samples in a 96 Well Plate for Testing Dose Response of Yeast RNA Pol I to Screened Ligands Using RT-PCR

	1	2	3	4	5	6	7	8	9	10	11	12
A	NTC for MEP2	Standard cDNA1/2 MEP2	Standard cDNA1/16 MEP2	Standard cDNA 1/2 HmrDNA	Standard cDNA1/16 HmrDNA	Sample Hmr 1562 nM Cerivastatin Sodium	Sample Hmr 390 nM Cerivastatin Sodium	Sample Hmr 1562 nM Aripirazole	Sample MEP2 2500 nM Agatroban	Sample MEP2 1562 nM Cerivastatin Sodium	Sample MEP2 6250 nM Aripirazole	Sample MEP2 780nM Aripirazole
B	NTC for MEP2	Standard cDNA1/2 MEP2	Standard cDNA1/16 MEP2	Standard cDNA1/4 HmrDNA	Standard cDNA1/16 HmrDNA	Sample Hmr 1562 nM Cerivastatin Sodium	Sample Hmr 6250 nM Aripirazole	Sample Hmr 1562 nM Aripirazole	Sample MEP2 2500 nM Agatroban	Sample MEP2 780 nM Cerivastatin Sodium	Sample MEP2 6250 nM Aripirazole	Sample MEP2 780nM Aripirazole
C	NTC for HmrDNA	Standard cDNA1/4 MEP2	Standard cDNA1/16 MEP2	Standard cDNA1/4 HmrDNA	Sample Hmr 2500 nM Agatroban	Sample Hmr 1562 nM Cerivastatin Sodium	Sample Hmr 6250 nM Aripirazole	Sample Hmr 780 nM Aripirazole	Sample MEP2 2500 nM Agatroban	Sample MEP2 780 nM Cerivastatin Sodium	Sample MEP2 3125 nM Aripirazole	Sample MEP2 780nM Aripirazole
D	NTC for HmrDNA	Standard cDNA1/4 MEP2	Standard cDNA 1× HmrDNA	Standard cDNA 1/4 HmrDNA	Sample Hmr 2500 nM Agatroban	Sample Hmr 780 nM Cerivastatin Sodium	Sample Hmr 6250 nM Aripirazole	Sample Hmr 780 nM Aripirazole	Sample MEP2 1250 nM Agatroban	Sample MEP2 780 nM Cerivastatin Sodium	Sample MEP2 3125 nM Aripirazole	Sample MEP2 Without Ligand
E	Standard cDNA 1× MEP2	Standard cDNA1/4 MEP2	Standard cDNA 1× HmrDNA	Standard cDNA1/8 HmrDNA	Sample Hmr 2500 nM Agatroban	Sample Hmr 780 nM Cerivastatin Sodium	Sample Hmr 3125 nM Aripirazole	Sample Hmr 780 nM Aripirazole	Sample MEP2 1250 nM Agatroban	Sample MEP2 390 nM Cerivastatin Sodium	Sample MEP2 3125 nM Aripirazole	Sample MEP2 Without Ligand
F	Standard cDNA 1× MEP2	Standard cDNA1/8 MEP2	Standard cDNA 1× HmrDNA	Standard cDNA1/8 HmrDNA	Sample Hmr 1250 nM Agatroban	Sample Hmr 780 nM Cerivastatin Sodium	Sample Hmr 3125 nM Aripirazole	Sample Hmr Without Ligand	Sample MEP2 1250 nM Agatroban	Sample MEP2 390 nM Cerivastatin Sodium	Sample MEP2 1562 nM Aripirazole	Sample MEP2 Without Ligand
G	Standard cDNA 1× MEP2	Standard cDNA1/8 MEP2	Standard cDNA 1/2 HmrDNA	Standard cDNA 1/8 HmrDNA	Sample Hmr 1250 nM Agatroban	Sample Hmr 390 nM Cerivastatin Sodium	Sample Hmr 3125 nM Aripirazole	Sample Hmr Without Ligand	Sample MEP2 1562 nM Cerivastatin Sodium	Sample MEP2 390 nM Cerivastatin Sodium	Sample MEP2 1562 nM Aripirazole	
H	Standard cDNA1/2 MEP2	Standard cDNA1/8 MEP2	Standard cDNA 1/2 HmrDNA	Standard cDNA1/16 HmrDNA	Sample Hmr 1250 nM Agatroban	Sample Hmr 390 nM Cerivastatin Sodium	Sample Hmr 1562 nM Aripirazole	Sample Hmr Without Ligand	Sample MEP2 1562 nM Cerivastatin Sodium	Sample MEP2 6250 nM Aripirazole	Sample MEP2 1562 nM Aripirazole	

```
Not3P64cDNA4_pHrP2FWD_Sample_Name=Not3P64cDNA4_pHrP2FWD_Chromat_id=8075959_Read_id=8002780_Version=1_Length=356  ----------NNNNNNNNNNNNNNNNNNNNNNNNNNNNNNNNNNNNNNACGCG
HumanrDNA_pHrP2                                                                                                   GCTGACACGCTGTCCTCTGGCGACCTGTCGCTGGAGAGGTTGGGCCTCCGGATGCGCGCG
                                                                                                                                                                                  ****

Not3P64cDNA4_pHrP2FWD_Sample_Name=Not3P64cDNA4_pHrP2FWD_Chromat_id=8075959_Read_id=8002780_Version=1_Length=356  GGGCTCTNGCCTACCGGTGACCCGGCTAGCCGGCCGCGCTCCTGCTTGAGCCGCCTGCCG
HumanrDNA_pHrP2                                                                                                   GGGCTCTGGCCTACCGGTGACCCGGCTAGCCGGCCGCGCTCCTGCTTGAGCCGCCTGCCG
                                                                                                                  ******* ******************************************************

Not3P64cDNA4_pHrP2FWD_Sample_Name=Not3P64cDNA4_pHrP2FWD_Chromat_id=8075959_Read_id=8002780_Version=1_Length=356  GGGCCCGCGGGCCTGCTGTTCTCTCGCGCGTCCGAGCGTCCCGACTCCCGGTGCCGGCCC
HumanrDNA_pHrP2                                                                                                   GGGCCCGCGGGCCTGCTGTTCTCTCGCGCGTCCGAGCGTCCCGACTCCCGGTGCCGGCCC
                                                                                                                  ************************************************************

Not3P64cDNA4_pHrP2FWD_Sample_Name=Not3P64cDNA4_pHrP2FWD_Chromat_id=8075959_Read_id=8002780_Version=1_Length=356  GGGTCCGGGTCTCTGACCCACCCGGGG-GCGGCGGGGAAGGCGGCGAGGGCCACCGTGCC
HumanrDNA_pHrP2                                                                                                   GGGTCCGGGTCTCTGACCCACCCGGGGGGCGGCGGGGAAGGCGGCGAGGGCCACCGTGCC
                                                                                                                  ************************** ***************************************

Not3P64cDNA4_pHrP2FWD_Sample_Name=Not3P64cDNA4_pHrP2FWD_Chromat_id=8075959_Read_id=8002780_Version=1_Length=356  CCCGTGCGCTCTCCGCTGCGGGCGCCCGGGGCGGCCGCGACAACCCCACCCCGCTGGCTC
HumanrDNA_pHrP2                                                                                                   CCCGTGCGCTCTCCGCTGCGGGCGCCCGGGGCGGCCGCGACAACCCCACCCCGCTGGCTC
                                                                                                                  ************************************************************

Not3P64cDNA4_pHrP2FWD_Sample_Name=Not3P64cDNA4_pHrP2FWD_Chromat_id=8075959_Read_id=8002780_Version=1_Length=356  CGTGCCGTGCGTGTCAGGCGTTCTCGTCTCCGCGGGGTTGTCCGCCGCCCCTTCCCCGGA
HumanrDNA_pHrP2                                                                                                   CGTGCCGTGCGTGTCAGGCGTTCTCGTCTCCGCGGGGTTGTCCGCCGCCCCTTCCCCGGA
                                                                                                                  ************************************************************

Not3P64cDNA4_pHrP2FWD_Sample_Name=Not3P64cDNA4_pHrP2FWD_Chromat_id=8075959_Read_id=8002780_Version=1_Length=356  GTGGGGGGTTGGCCGGAGCCGATN   356
HumanrDNA_pHrP2                                                                                                   GTGGGGGGTTGGCCGGAGCCGATC   384
                                                                                                                  **********************
```

Appendix M Sequence Alignment of DNA from YBR140C-HmrDNA Strain with Human rDNA Sequence from pHrP2 Plasmid

REFERENCES

(1) Kim, M. J., Xia, B.; Suh, H. N.; Lee, S. H.; Jun, S.; Lien, E. M.; Zhang, J.; Chen, K.; Park, J. I. PAF-Myc-Controlled Cell Stemness is Required for Intestinal Regeneration and Tumorigenesis. *Dev. Cell.* **2018**, *44*, 582-596.
(2) Corbineau, S., Lassalle, B.; Givelet, M.; Souissi-Sarahoui, I.; Firlej, V.; Romeo, P. H.; Allemand, I.; Riou, L.; Fouchet, P. Spermatogonial Stem Cells and Progenitors are Refractory to Reprogramming to Pluripotency by the Transcription Factors Oct3/4, c-Myc, Sox2 and Klf4. *Onco. Target.* **2017**, *8*, 10050-10063.
(3) Zhao, Y., Huang, X.; Ding, T. W.; Gong, Z. Enhanced Angiogenesis, Hypoxia and Neutrophil Recruitment During Myc-Induced Liver Tumorigenesis in Zebrafish. *Scientific Reports* **2016**, *6*.
(4) Ji, H., Wu, G.; Zhan, X.; Nolan, A.; Koh, C.; De Marzo, A.; Doan, H. M.; Fan, J.; Cheadle, C.; Fallahi, M. Cell-Type Independent MYC Target Genes Revealed a Primordial Signature Involved in Biomass Accumulation. *PloS One* **2011**, *6*, e26057.
(5) Roeder, R. G., Rutter, W. J. Multiple forms of DNA-Dependent RNA Polymerase in Eukaryotic Organisms. *Nature* **1969**, *224*, 234-237.
(6) Kulkens, T., Riggs, D. L.; Heck, J. D.; Planta, R. J.; Nomura, M. The Yeast RNA Polymerase I Promoter: Ribosomal DNA Sequences Involved in Transcription Initiation and Complex Formation in Vitro. *Nucleic. Acids. Research.* **1991**, *19*, 5363–5370.
(7) Nomura, M., Nogi, Y.; Yano, R.; Oakes, M.; Keys, D. A.; Dodd, L. V. A. RNA Polymerase I, the Nucleolus and Synthesis of 35S rRNA in the Yeast Saccharomyces Cerevisiae. *Nature* **1969**, *224*, 234–237.
(8) Ferna ́ndez-Tornero, C., Moreno-Morcillo. Marı´a.; Rashid, U. J.; Taylor, N. M. I.; Ruiz, F. M.; Gruene, T.; Legrand, P.; Steuerwald, U.; Muller, C. W. Crystal Structure of the 14-Subunit RNA Polymerase I. *Nature* **2013**, *502*, 644–649.
(9) Cramer, P., Bushnell, D. A.; Kornberg, R. D. Structural Basis of Transcription: RNA Polymerase II at 2.8 Angstrom Resolution. *Science* **2001**, *292*, 1863–1876.
(10) Dammann, R., Lucchini, R.; Koller, T.; Sogo, J. M. Transcription in the Yeast rRNA Gene Locus: Distribution of the Active Gene Copies and Chromatin Structure of Their Flanking Regulatory Sequences. *Mol Cell Biol*
1995, *15*, 5294-5303.
(11) Ghoshal, K., Majumder, S.;, Datta, J.; Motiwala, T.; Bai, S.; Sharma, S. M.; Frankel, W.; Jacob, S. T. Role of Human Ribosomal RNA (rRNA) Promoter Methylation and of Methyl-CpG-binding Protein MBD2 in the Suppression of rRNA Gene Expression. *The Journal of Biological Chemistry* **2004**, *279*, 6783-6793.
(12) Clos, J., Normann, A.; Ohrlein, A.; Grummt, I. The Core Promoter of Mouse rDNA Consists of Two Functionally Distinct Domains. *Nucleic Acids Res* **1986**, *14*, 7581-7595.
(13) Reeder, R. H. Enhancers and Ribosomal Gene Spacers. *Cell* **1984**, *38*, 349-351.
(14) Kuhn, A., Grummt, I. A Novel Promoter in the Mouse rDNA Spacer is Active In Vivo and In Vitro. *EMBO Journal* **1987**, *6*, 3487-3492.
(15) Comai, L. Mechanism of RNA Polymerase I Transcription. *Advances. in. Protein. Chemistry.* **2004**, *67*, 123-155.
(16) Engel, C., Plitzko, J., Cramer, P. RNA Polymerase I-Rrn3 Complex at 4.8 A Resolution. *Nature Communication* **2016**, *7*, e12129.

(17) Russell, J., Zomerdijk, J.C. The RNA Polymerase I Transcription Machinery. *Biochem Soc Symp* **2006**, *73*, 203–216.
(18) Peyroche, G., Levillain, E.; Siaut, M.; Callebaut, I.; Schultz, P.; Sentenac, A.; Riva, M.; Carles, Christophe. The A14–A43 Heterodimer Subunit in Yeast RNA pol I and Their Relationship to Rpb4–Rpb7 Pol II Subunits. *Proc Natl Acad Sci USA* **2002**, *99*, 14670–14675.
(19) Tuske S., S. S. G. W. X. H. B. S. E. M., J.; Birktoft, J. J.; Leroy, O.; Ismail, S.; Clark, A. D. Jr. Inhibition of Bacterial RNA Polymerase by Streptolydigin: Stabilization of a Straight-Bridge-Helix Active-Center Conformation. *Cell* **2005**, *122*, 541–552.
(20) Tafur, L., Sadian, Y.; Hoffmann, N. A.; Jakobi, A. J.; Wetzel, R.; Hagen, W. J. H.; Sachse, Carsten.; Müller, Christoph. W. Molecular Structures of Transcribing RNA Polymerase I. *Molecular Cell* **2016**, *64*, 1135-1143.
(21) Whitesell, L., Lindquist, S. Inhibiting the Transcription Factor HSF1 as an Anticancer Strategy. *Expert Opin Ther Targets* **2009**, *13*, 469-478.
(22) Liebhaber, S. A., Wolf, S.; Schlessinger, D. Differences in rRNA Metabolism of Primary and SV40-Transformed Human Fibroblasts. *Cell* **1978**, *13*, 121-127.
(23) Hadjiolov, A. A.: *The Nucleolus and Ribosome Biogenesis. Cell Biology Monographs*; Springer-Verlag: New York, 1985; Vol. 12.
(24) Bywater, M. J., Poortinga, C.; Sanij, E.; Hein, N.; Peck, A.; Cullinane, C.; Wall, M.; Cluse, L.; Drygin, D.; Anderes, K.; Huser, N.; Proffitt, C.; Bliesath, J.; Haddach, M.; Schwaebe, M. K.; Ryckman, D. M.; Rice, W. G.; Schmitt, C.; Hannan, R. D. Inhibition of RNA Polymerase I as a Therapeutic Strategy to Promote Cancer-Specific Activation of P53. *Cancer Cell* **2012**, *22*, 51-65.
(25) Colis, L., Ernst G.; Sanders, S.; Liu, H.; Sirajuddin, P.; Peltonen, K.; DePasquale, M.; Barrow, J. C.; Laiho, M. Design, Synthesis, and Structure-Activity Relationships of Pyridoquinazolinecarboxamides as RNA Polymerase I Inhibitors. *J Med Chem* **2014**, *57*, 4950-4961.
(26) Cramer, P., Armache, K.J.; Baumli, S.; Benkert, S.; Brueckner, F.; Buchen, C.; Damsma, G. E.; Dengl, S.; Geiger, S. R.; Jasiak, A. J.; Jawhari, A.; Jennebach, S.; Kamenski, T.; Kettenberger, H.; Kuhn, C. D.; Lehmann, E.; Leike, K.; Sydow, J.F.; Vannini, A. Structure of Eukaryotic RNA Polymerases. *Annu Rev Biophys* **2008**, *37*, 337-352.
(27) Drygin, D., Lin, A.; Bliesath, J.; Ho, C. B.; O'Brien, S. E.; Proffitt, C.; Omori, M.; Haddach, M.; Schwaebe, M. K.; Siddiqui-Jain, A.; Streiner, N.; Quin, J. E.; Sanij, E.; Bywater, M. J.; Hannan, R. D.; Ryckman, D.; Anderes, K.; Rice, W. G. Targeting RNA Polymerase I with an Oral Small Molecule CX-5461 Inhibits Ribosomal RNA Synthesis and Solid Tumor Growth. *Cancer Res* **2011**, *71*, 1418-1430.
(28) Harris, C. C. The Carcinogenicity of Anticancer Drugs: a Hazard in Man. *Cancer Cell* **1976**, *37*, 1014-1023.
(29) Heix, J., Grummt, I. Species Specificity of Transcription by RNA Polymrase I. *Curr Opin Genet Dev* **1995**, *5*, 652-656.
(30) Yamamoto, K., Koga, A.; Yamamoto, M.; Nishi, Y.; Tamura, T.; Nogi, Y.; Muramatsu, M. Identification of a Novel 70 kDa Protein that Binds to the Core Promoter Element and is Essential for Ribosomal DNA Transcription. *Nucleic Acids Res* **2000**, *28*, 1199-1205.

(31) Moss , T., Stefanovsky, V. Y. At the Center of Eukaryotic Life. *Cell* **2002**, *109*, 545-548.
(32) Chen, S., Seiler, J.; Santiago-Reichelt, M.; Felbel, K.; Grummt, I.; Voit, R. Repression of RNA Polymerase I Upon Stress is Caused by Inhibition of RNA-Dependent Deacetylation of PAF53 by SIRT7. *Molecular Cell* **2013**, *52*, 303–313.
(33) Yamamoto, R. T., Nogi, Y.; Dodd, J. A.; Nomura, M. RRN3 Gene of Saccharomyces Cerevisiae Encodes an Essential RNA Polymerase I Transcription Factor Which Interacts with the Polymerase Independently of DNA Template. *E M B O J* **1996**, *15*, 3964–3973.
(34) Russell, J., Zomerdijk, J. C. B. M. RNA-Polymerase-I-Directed rDNA Transcription, Life and Works. *Trends Biochem Sci* **2005**, *30*, 87-96.
(35) Blattner, C., Jennebach, S.; Herzog, F.; Mayer, A.; Cheung, A. C. M.; Witte, G.; Lorenzen, K.; Hopfner, K.; Aebersold, R.; Cramer, P. Molecular Basis of Rrn3-Regulated RNA Polymerase I Initiation and Cell Growth. *Gene Dev* **2011**, *25*, 2093-2105.
(36) Shoemaker, R. H., Monks, A.; Alley, M. C.; Scudiero, D. A.; Fine, D. L.; McLemore, T. L.; Abbott, B. J.; Paull, K. D.; Mayo, J. G.; Boyd, M. R. Development of Human Tumor Cell Line Panels for Use in Disease-Oriented Drug Screening. *Prog Clin Biol Res* **1988**, *276*, 265-286.
(37) Shoemaker, R. H. The NCI60 Human Tumour Cell Line Anticancer Drug Screen. *Nat Rev Cancer* **2006**, *6*, 813-823.
(38) Puck, T. T., Fisher, H. W. Genetics Of Somatic Mammalian Cells : I. Demonstration Of The Existence Of Mutants With Different Growth Requirements In a Human Cancer Cell Strain (Hela). *J Experimental Medicine* **1956**, *104*, 427-434.
(39) Adams, J. M., Harris, A. W.; Pinkert, C. A.; Corcoran, L. M.; Alexander, W. S.; Cory, S.; Palmiter, R. D.; Brinster, R. L. The c-Myc Oncogene Driven by Immunoglobulin Enhancers Induces Lymphoid Malignancy in Transgenic Mice. *Nature* **1985**, *318*, 533-538.
(40) Kurl, R. N., Rothblum, L. I.; Jacob, S. T. A Purified Fraction Containing RNA Polymerase I that Can Accurately Transcribe rat Ribosomal RNA Gene. *Proc Natl Acad Sci U S A* **1984**, *81*, 6672–6675.
(41) Drygin, D., Lin, A.; Bliesath, J.; Ho, C. B.; O'Brien, S. E.; Proffitt, C.; Omori, M.; Haddach, M.; Schwaebe, M. K.; Siddiqui-Jain, A.; Streiner, N.; Quin, J. E.; Sanij, E.; Bywater, M. J.; Hannan, R. D.; Ryckman, D.; Anderes, K.; Rice, W. G. Targeting RNA Polymerase I with an Oral Small Molecule CX-5461 Inhibits Ribosomal RNA Synthesis and Solid Tumor Growth. *Cancer Res* **2011**, *71*, 1418-1430.
(42) Andrews, W. J., Panova, T.; Normand, C.; Gadal, O.; Tikhonova, I. G.; Panov, K. I. Old Drug, New Target: Ellipticines Selectively Inhibit RNA Polymerase I Transcription. *J Biol Chem* **2013**, *288*, 4567-4582.
(43) Peltonen, K. C., L.; Liu, H.; Trivedi, R.; Moubarek, M. S.; Moore, H. M.; Bai, B.; Rudek, M. A.; Bieberich, C. J.; Laiho, M. A targeting modality for destruction of RNA polymerase I that possesses anticancer activity. *Cancer Cell* **2014**, *25*, 77-90.
(44) Roger, B., Moisand. A.; Amalric. F.; Bouvet. P. Repression of RNA Polymerase I Transcription by Nucleolin is Independent of the RNA Sequence that is Transcribed. *J Biol Chem* **2002**, *277*, 10209-10219.
(45) Botstein, D., Fink, G. R. Yeast: An Experimental Organism for Modern Micrology. *Science* **1988**, *240*, 1439–1443.

(46) Powers, S., Kataoka, T.; Fasano, O.; Goldfarb, M.; Strathern, J.; Broach, J.; Wigler, M. Genes in S. Cerevisiae Encoding Proteins with Domains Homologous to the Mammalian Ras Proteins. *Cell* **1984**, *36*, 607-612.
(47) Mokdad-Gargouri, R., Belhadj, K.; Gargouri, A. Translational control of Human p53 Expression in Yeast Mediated by 5'-UTR-ORF Structural Interaction. *Nucleic Acids Res* **2001**, *29*, 1222–1227.
(48) Nomura, M., Nogi, Y.; Yano, R.; Oakes, M.; Keys, D. A.; Dodd, L. V. A. RNA Polymerase I, the Nucleolus and Synthesis of 35S rRNA in the Yeast Saccharomyces Cerevisiae. *The Translational Apparatus* **1993**, *9*, 89-99.
(49) Seither, P., Grummt, I. Molecular Cloning of RPA2, the Gene Encoding the Second Largest Subunit of Mouse RNA Polymerase I. *Genomics* **1996**, *37*, 135-139.
(50) Lacroute, F. Regulation of Pyrimidine Biosynthesis in Saccharomyces Cerevisiae. *Bacteriol J* **1968**, *95*, 824-832.
(51) Umezu, K., Amaya, T.; Yoshimoto, A.; Tomita, K. Purification and Properties of Orotidine-5'-Phosphate Pyrophosphorylase and Orotidine-5'-Phosphate Decarboxylase from Baker's Yeast. *J Biochem* **1971**, *70*, 249-262.
(52) Klinner, U., Sch€afer, B. Genetic Aspects of Targeted Insertion Mutagenesis in Yeasts. *FEMS Microbiology Reviews* **2004**, *28*, 201–223.
(53) Lee, A. Y., St.Onge, R. P.; Proctor, M. J.; Wallace, I. M.; Nile, A. H.; Spagnuolo, P. A.; Jitkova, Y.; Gronda, M.; Wu, Y.; Kim, M. K.; Cheung-Ong, K.; Torres, N. P.; Spear, E. D.; Han, M. K. L.; Schlecht, U.; Suresh, S.; Duby, G.; Heisler, L. E.; Surendra, A.; Fung, E.; Urbanus, M. L.; Gebbia, M.; Lissina, E.; Miranda, M.; Chiang, J. H.; Aparicio, A. M.; Zeghouf, M.; Davis, R. W.; Cherfils, J.; Boutry, M.; Kaiser, C. A.; Cummins, C. L.; Trimble, W. S.; Brown, G. W.; Schimmer, A. D.; Bankaitis, V. A.; Nislow, C.; Bader, G. D.; Giaever, G. Mapping the Cellular Response to Small Molecules Using Chemogenomic Fitness Signatures. *Science* **2014**, *344*.
(54) Horuchi, T., Horiuchi, S.; Mizuno, D. A possible Negative Feedback Phenomenon Controlling Formation of Alkaline Phosphomonoesterase in Escherichia coli. *Nature* **1959**, *183*, 1529-1530.
(55) Sun, Y., Sun, T. L.; Huang, H. W. Physical Properties of Escherichia coli Spheroplast Membranes. *Biophys J* **2014**, *107*, 2082–2090.
(56) Masek, T., Vopalensky, V.; Suchomelova, P.; Pospisek, M. Denaturing RNA Electrophoresis in TAE Agarose Gels. *Anal Biochem* **2005**, *336*, 46-50.
(57) Wang, X. W., Seed, B. A PCR Primer Bank for Quantitative Gene Expression Analysis. *Nucleic Acids Research* **2003**, *31*, e154.
(58) Marini, A. M., Soussi-Boudekou, S.; Vissers, S.; Andre, B. A Family of Ammonium Transporters in Saccharomyces Cerevisiae. *Mol Cell Biol* **1997**, *17*, 4282-4293.
(59) Lorenz, M. C., Heitman, J. The MEP2 Ammonium Permease Regulates Pseudohyphal Differentiation in Saccharomyces Cerevisiae. *EMBO Journal* **1998**, *17*, 1236-1247.
(60) Ilan. J., I., J.; Quastel, J. H. Effects of Actinomycin D on Nucleic Acid Metabolism and Protein Biosynthesis During Metamorphosis of Tenebrio Molitor L.Biochem. J. 1966. 100. 2. 441-447. Effects of Actinomycin D on Nucleic Acid Metabolism and Protein Biosynthesis During Metamorphosis of Tenebrio Molitor L. *Biochem J* **1966**, *100*, 441-447.

(61) Kirk, J. M. The Mode of Action of Actinomycin D. *Biochinmica Biophysica Acta* **1960**, *42*, 167-169.
(62) Livak, K. J., Schmittgen,Thomas D. Analysis of Relative Gene Expression Data Using RealTime Quantitative PCR and the 22DDCT Method. *Methods* **2001**, *25*, 402-408.
(63) Fried, M. G. Measurement of Protein-DNA Interaction Parameters by Electrophoresis Mobility Shift Assay. *Electrophoresis* **1989**, *10*, 366-376.
(64) Dias, R. S., Carmo, L.S.; Heneine, L. G. D.; Rocha, P. H.; Barbosa, C. F.; Rodrigues R. J., Linardi, V. R The Use of Mice as Animal Model for Testing Acute Toxicity (LD-50) of Toxic Shock Syndrome Toxin. *Arq Bras Med Vet Zootec* **2009**, *61*, 170-173.

VITA

Student Name: Xiao Tan

Place of Birth: Zhengzhou, Henan China

Educational Institutions and Degrees Already Awarded

Henan University of Technology: Bachelor's Degree of Engineering

University of North Carolina at Greensboro: Master's Degree of Science

Professional Position Held

QC Analyst at Catalent Pharma Solutions (2018-Present)

Professional Publications

A Cell Based Screening System for RNA Polymerase I Inhibitors. MedChemComm. 2019 (Submitted)